

Effective theories for nuclei at high energies

Oscar Garcia-Montero^{1*} and Sören Schlichting^{1†}

¹Fakultät für Physik, Universität Bielefeld, Universitätsstraße 25,
Bielefeld, D-33615, Germany.

*Corresponding author(s). E-mail(s): garcia@physik.uni-bielefeld.de;

Contributing authors: sschlichting@physik.uni-bielefeld.de;

†These authors contributed equally to this work.

Abstract

We discuss the application of the Color Glass Condensate (CGC), an effective field theory of Quantum Chromodynamics (QCD), to describe high-energy nuclear interactions. We first provide an introduction to the methods and language of the CGC, its role in understanding gluon saturation in heavy-ion collisions at the LHC and RHIC, and its relevance in various scattering processes such as Deep Inelastic Scattering (DIS). The application of the CGC effective field theory to describe hadron-hadron collisions is discussed in the scope of asymmetric *dilute-dense* collisions, and Heavy-Ion Collisions in the *dense-dense* limit. The review covers theoretical foundations, recent advancements, and phenomenological applications, focusing on using the CGC to determine the initial conditions of heavy-ion collisions.

Keywords: Color-Glass Condensate, Saturation, Deep-Inelastic Scattering, Heavy-Ion Collisions, Nuclear Structure, Forward physics

1 Introduction

High-energy heavy-ion collisions at the Large Hadron Collider (LHC), and the Relativistic Heavy Ion Collider (RHIC) offer a unique window into the properties of nuclei at high energies and the behavior of nuclear matter under extreme conditions. Clearly, at such high energies, low-energy descriptions of atomic nuclei based solely on nucleons and mesons become inapplicable, giving way to other effective theories of Quantum Chromodynamics (QCD) that capture the emergent phenomena and interactions of quarks and gluons within the nuclear medium. Nevertheless, at the scales at which

nuclear structure manifests itself, the theory of strong interactions remains strongly coupled and highly non-perturbative. Hence, to describe the relevant properties of nuclei at high-energies, effective theories based on the principles and symmetries of QCD have been developed. Such is the case of the Color Glass Condensate [1–4], an effective theory of QCD in high-energy scattering processes.

Based on the fundamental degrees of freedom of QCD, the CGC accounts for the rich interplay between linear production and non-linear absorption of gluons, which marks the onset of collective gluon dynamics in the boosted nucleus and describes the phenomenon of gluon saturation as an emergent property. The scope of this review is to provide a pedagogical introduction to the CGC effective theory, and its applications to Deeply Inelastic electron-proton $e + p$ and electron-nucleus $e + A$ Scattering (DIS) and hadronic proton-proton $p + p$, proton-nucleus $p + A$ and nucleus-nucleus $A + A$ collisions. Below, in the remainder of this section, we lay out the basic concepts of high-energy scattering in which the CGC effective theory is framed.

Subsequently, in Sec. 2, we sketch the basic theoretical ideas underlying the CGC, and discuss the application to DIS in Sec. 3. We proceed by summarizing the advances and status quo of the CGC in the context of hadronic collisions in Sec. 4, where in Sec. 4.1 we focus on the so-called dilute dense limit, e.g. used in the case of forward particle production in p+A collisions, while in Sec. 4.2 we describe the dense-dense limit, usually employed to calculate the initial conditions for the space-time of the medium created in heavy-ion collisions. We conclude this review in Sec. 5.

1.1 High energy scattering in QCD

The fundamental subnucleonic degrees of freedom of hadrons, quarks and gluons, create a rich substructure inside nuclei, manifested by a complex many-body nucleonic (nuclear) QCD wavefunction. High-energy scattering experiments such as DIS are used to access this partonic QCD content. The information of the nuclear wavefunction can be understood in terms of correlation functions of (anti-)quark Ψ fields and gluon field-strength operators, $F_a^{\mu\nu}$. Such QCD correlation functions are in general very complex, as they reflect all the information about the configurations of colored particles inside hadrons or nuclei. Nevertheless, there are well established theoretical and experimental formulations for two-point correlations functions, such as collinear parton distribution functions (PDFs), Transverse Momentum Distributions (TMDs), Generalized Parton Distribution Functions (GPDs), Wigner Distributions, and we refer to [5–8] for dedicated reviews on the subject. The simplest case is the collinear gluon PDF $f_{g/h}(x, \mu^2)$ inside a hadron/nucleus h , given by

$$f_{g/h}(x, \mu^2) = \int \frac{dy^-}{2\pi} \frac{e^{-ixP_h^+ y^-}}{xP_h^+} \langle P_h^+, \mathbf{0}_T | F_a(0, y^-, \mathbf{0}_T)^{\nu+} \mathcal{O}^{ab} F_b(0, 0, \mathbf{0}_T)^+ | P_h^+, \mathbf{0}_T \rangle_{\overline{MS}}, \quad (1)$$

which describes the distribution of gluons with (light-cone) momentum fraction $x = p_g^+/P_h^+$, measured at a renormalization scale μ^2 . The integration is performed along the light-cone position y^- , conjugate to the light-cone momentum P^+ . In what follows, we will be using the light cone positions and momenta, which are defined by $x^\pm = (t \pm z)/\sqrt{2}$ and $p^\pm = (p_0 \pm p_z)/\sqrt{2}$, respectively. In a collinear PDF there is no information

on the intrinsic transverse momentum of the gluons, since the field-strength correlator is integrated over transverse momenta, i.e. the gluonic field strength is measured at the same transverse position $\mathbf{0}_T$. This is different for a TMD, where this information is retained [8]. Similarly GPDs retain information about the spatial position of partons inside hadrons [9], and Wigner Distributions retain information about position and momentum [7, 10]. Irrespective of this, it is important to note that all PDFs, TMDs, GPDs, only contain information on single parton distributions and do not encapsulate the full extent of the many-body complexity of the nuclear wavefunction.

Due to the non-perturbative nature of QCD bound states, QCD correlation functions such as TMDs and PDFs, cannot be computed from first principles in perturbative QCD. Such non-perturbative knowledge has been historically extracted from fits to observables measured in experiments such as DIS at the HERA collider at DESY, Hamburg and the Thomas Jefferson National Accelerator Facility (JLAB). More modern extractions perform a simultaneous extraction including also data from hadronic collisions such as jet, high- k_T charmed meson, and electromagnetic probe data [11]. Theoretical advances and algorithmic improvements in lattice QCD, can also help to provide additional theoretical insight into the behavior of these non-perturbative QCD correlation functions. For a recent review on this rapidly evolving field, we refer to Ref. [12].

1.1.1 Kinematics

To gain a more intuitive understanding of the partonic content of hadrons and nuclei, it is insightful to consider a high-energy scattering experiment, such as DIS, where a probe interacts with the partons inside hadrons, exchanging four-momentum q in the process. Generally speaking, the kinematics of this process can be described in terms of the center-of-mass (CoM) energy \sqrt{s} , the virtuality of the photon, $Q^2 = -q^2$, and the Bjorken scaling variable x . Intuitively, Q provides a *resolution scale* for the partonic content of the hadron, while one can relate x , in single parton kinematics, to the momentum fraction carried by the interacting parton. Additionally, x is related to the inelasticity of the process $y = Q^2/sx$.

Different regions in the (x, Q^2) phase-space, can then be accessed depending on the detailed kinematics of the scattering experiment. For a fixed center-of-mass energy, more massive final states (e.g. Z -bosons) sample regions of larger x , whereas higher center-of-mass energies give access to smaller values of x . Generally, one finds that at typical values of $Q^2 \sim \text{GeV}^2$, hadrons consist of a small number of large $x \sim 1$ valence partons, and a large number of sea partons with momentum fractions $x \ll 1$.

Even though the property of asymptotic freedom guarantees that the underlying QCD interactions can be treated perturbatively at high momentum transfer, the complex partonic structure of hadrons and nuclei and the non-linear nature of gluon interactions make a general description of high-energy scattering processes intractable. Depending on the kinematic regime that is being probed, different theoretical formalisms/expansion schemes in QCD can then be used to describe the process. The traditional and most well established description of perturbative QCD, known as collinear factorization, describes scattering events comprised of small numbers of hard

scatterings of partons by approximating the hadronic cross sections in terms of a convolution of partonic cross sections with the non-perturbatively extracted collinear PDFs. The separation of non-perturbative dynamics inside the hadron and the perturbative dynamics of partonic scattering, is known in the literature as the *factorization theorem*, which exploits a separation of scales that also allows one to express the scattering processes in terms of scatterings of a few partons. While the separation of nucleonic and partonic scales guarantees a good theoretical control, it also means that there is a priori no connection to low energy nuclear structure, e.g. the spatial distribution of nucleons in nuclei. Evidently, the pQCD approach requires small values of the coupling constant of QCD, $\alpha_S(Q^2) \ll 1$; however due to the limitation to a small number of partonic scatterings the range of applicability of this approach is also limited to large/moderate values of x , where hadronic structure is dominated by few partons.

1.2 Gluon saturation and the Color Glass Condensate

Conversely, when $x \ll 1$ (i.e. low- x) the collinear parton distributions of gluons and sea-quarks increase according to a power law $\sim x^{-a(Q^2)}$, due to the radiative emissions of soft gluons, carrying a small fraction of the hadron's momentum. Naturally, the conventional perturbative description breaks down when gluon densities become non-perturbatively large $\sim 1/\alpha_S$, and new effective descriptions of QCD are needed to account for the multi-particle dynamics inside the hadron. While in principle there are different possibilities to account for the ensuing non-linear QCD dynamics, we will focus on the Color Glass Condensate effective field theory of high-energy QCD, which provides a weak coupling description of high-energy scattering processes, in the multi-parton regime at low- x .

Clearly, one of the most remarkable features of the Color Glass Condensate Effective Field Theory is that it predicts the feature of perturbative gluon saturation in hadrons and nuclei. While in the few parton regime, the evolution of parton densities towards smaller values of x can be calculated perturbatively and gives rise to the linear BFKL evolution [13–15], the phase-space density of gluons increases with decreasing x due to successive radiative emissions. Consequently, at small- x , gluons densely populate the available phase-space, and it becomes increasingly likely for gluons to recombine -or fuse-, leading to a non-linear evolution of the parton densities, as encoded in the BK/JIMWLK evolution equations of small- x QCD [16–22]. Eventually, the balance between radiative gluon emission and recombination leads to a saturation of the gluon density in the multi-parton regime at small- x .

More precisely, the interplay between radiative emissions and absorptions creates an effective semi-hard scale, $Q_s(x)$, which serves as a dynamical scale separating the two regimes. Specifically, for transverse momenta, $k_T < Q_s$, the gluon distribution is saturated while gluons with higher transverse momenta, $k_T > Q_s$ are still dilute in phase space. Clearly, the saturation scale $Q_s(x)$ is a dynamical scale as it is controlled by the variable x , where phenomenologically it has been found that $Q_s^2(x) \sim x^{-\lambda}$, with $\lambda \approx 0.2 - 0.3$ [23]. Since the nucleon density affects the saturation scale, larger nuclei become saturated already at lower energies, and the saturation scale $Q_{s,A}$ in nuclei is enhanced compared to the $Q_{s,Ap}$ saturation scale in a proton, as $Q_{s,A}^2 \sim$

$A^{1/3}Q_{s,p}^2$ [2, 3]. Hence, the Color Glass Condensate framework is particularly well suited for an effective description of nuclei at high-energies, where a larger fraction of gluons have transverse momenta $k_T \lesssim Q_s$ and we will discuss its phenomenological applications in Sec. 3 and 4.

2 Effective theory for high-energy QCD – Color Glass Condensate

Basics: Despite the fact that due to their complicated partonic structure the scattering of QCD bound states represents a highly complicated process, even at asymptotically high energies, it is instructive to follow Bjorken [24] and first consider the much simpler process of high-energy scattering of partons. We picture a process where an incoming quark with large momentum interacts with the color field of the target. In the laboratory frame we can set the incoming quark to be moving to the right and the target to be moving to the left, both at almost the speed of light, as illustrated in Fig. 1. Due to Lorentz contraction, the influence of the color fields of the target is then confined to a narrow region around $x^+ = \frac{t+z}{\sqrt{2}} = 0$. Similarly, due to time dilation, the color fields of the target appear as quasi-static i.e. approximately $x^- = \frac{t-z}{\sqrt{2}}$ independent fields, such that if we adapt an appropriate gauge choice and view the color field as emerging from individual color charges, with density $\rho^a(x^+, x_T)$, the color field of the target can be expressed as [25]

$$A^-(x^+, x_T) = \frac{1}{-\Delta_\perp} g\rho^a(x^+, x_T)t^a \quad (2)$$

with field-strength $F^{i-}(x^+, x_T) = \partial^i A^-(x^+, x_T)$ localized around $x^+ \sim 0$, where x^+ can be viewed as a time variable in the process. The operator Δ_\perp corresponds to the inverse transverse gluon propagator, and therefore, acting with its inverse is equivalent with a convolution with the transverse gluon propagator. Since the interaction of projectile and target only takes place around $x^+ \simeq 0$, the incoming/outgoing quark propagates in the vacuum before ($x^+ < 0$) and after ($x^+ > 0$) the interaction with the color field of the target, and the non-trivial part of the calculation is to relate the fermion field $\Psi(x^+ = 0^+, x^-, \mathbf{x}_T)$ after the interaction ($x^+ = 0^+$) to the incoming field $\Psi(x^+ = 0^-, x^-, \mathbf{x}_T)$. By treating the problem to lowest order in perturbation theory, the interaction of the quark with the target is then described by the solution of the Dirac equation $(i\cancel{D} - m)\Psi(x) = 0$, which to leading order in the eikonal approximation takes the form

$$(\partial_+ - igA^-(x))\Psi^-(x) = 0, \quad (3)$$

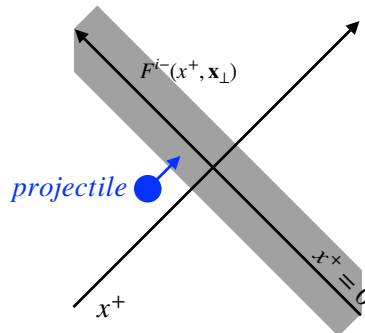


Fig. 1 Space-time picture of high-energy scattering

for the relevant light cone component $\Psi^- = \frac{1}{2}\gamma^-\gamma^+\Psi$ of the Dirac field (see e.g. [4] for details). The solution of Eq. (3),

$$\Psi^-(x^+ = 0^+, x^-, \mathbf{x}_T) = V(\mathbf{x}_T)\Psi^-(x^+ = 0^-, x^-, \mathbf{x}_T) \quad (4)$$

shows that high-energy scattering processes in QCD are described by light-like Wilson lines,

$$V(\mathbf{x}_T) = \mathcal{P} \exp \left[ig \int_{-\infty}^{\infty} dz^+ A^-(z^+, \mathbf{x}_T) \right], \quad (5)$$

which characterize the eikonal propagation of color charges. By performing a Fourier analysis of the incoming and outgoing quark field, we immediately see that – in addition to a color rotation – the light-like Wilson line $V(x_T)$ characterizes the transverse momentum transfer to the quark, as

$$\Psi^-(x^+ = 0^+, x^-, \mathbf{p}_T) = \int \frac{d^2\mathbf{q}_T}{(2\pi)^2} \tilde{V}(\mathbf{q}_T)\Psi^-(x^+ = 0^-, x^-, \mathbf{p}_T - \mathbf{q}_T) \quad (6)$$

such that the momentum \mathbf{p}_T of the outgoing quark is given by the sum of the incoming momentum $\mathbf{p}_T - \mathbf{q}_T$ and the momentum transfer \mathbf{q}_T from the target. Since the Wilson-line $V(x_T)$ contains an infinite number of gauge field insertions, it re-sums the transverse momentum transfer encountered in multiple interactions with the target, while neglecting the longitudinal momentum transfer in all interactions [26]. Conversely, in the dilute limit, where the Wilson line can be expanded around $V(\mathbf{x}_T) = \mathbb{I}$, one can recover the high-energy limit of the standard perturbative QCD result¹ (see Refs. [27–31] and references therein).

Despite the simplistic nature of the above example, it serves as a good illustration of the underlying physics. Hence, the general strategy of perturbative QCD (pQCD) calculations is to separate the dynamics of the partonic sub-process from genuinely non-perturbative information such as the distribution of incoming quarks in a hadronic bound state. In this case, such partonic dynamics would be the high-energy scattering of the quark with the color field of the target. By supplementing the required non-perturbative information, about a) the (momentum-) distribution of partons inside the projectile in form of a collinear PDF and b) the correlation functions of light-like Wilson lines inside the target, the above expressions can thus be turned into a leading order cross-section calculation for forward particle production, as discussed in Sec. 4.1.

In this spirit, the Color-Glass Condensate (CGC) is an effective theory for high-energy scattering based on light-like Wilson lines as fundamental degrees of freedom. Generically, the computational strategy is to compute observables, such as production cross-sections or particle production yields, in the presence of an individual realization of the Wilson lines $V(\mathbf{x})$ of a dense hadronic object. Subsequently, one performs a statistical average over all possible realizations of the Wilson lines $V(\mathbf{x})$, as described

¹Note that in the high-energy limit, the longitudinal momenta are large and the small longitudinal momentum transfer that is included in the pQCD calculation can be neglected. The calculation sketched above, is directly performed in the high-energy limit and neglects longitudinal momentum transfer from the very beginning.

by a weight functional $W_x[V]$

$$\langle \mathcal{O} \rangle_x = \int DV \mathcal{W}_x[V] \mathcal{O}[V] \quad (7)$$

Generally speaking, the weight functional $W_x[V]$ encodes information about correlated scattering of multiple highly energetic partons, and is not known a priori. Moreover, since this theoretical description requires a hitherto arbitrary separation into gluon fields that generate the Wilson lines, and dynamical gluons which enter perturbative calculation of matrix elements, there is a requirement that cross-sections are invariant under a change of this separation scale. This process gives rise to the JIMWLK evolution equation [19, 20, 32–34], which describes the evolution of the weight functional $W_x[V]$ with decreasing momentum fraction x or increasing center-of-mass energy for fixed kinematics.

By now the most frequently adopted strategy is thus to develop a physically motivated model for the weight functional at an initial scale, typically $x_0 \sim 0.1$, calculate its evolution with decreasing x based on JIMWLK (or BK) evolution, and constrain the parameters of the model by fits to deep inelastic scattering or hadronic collision data. By asserting universality of the CGC weight function, the same theoretical framework and model can then be used to provide a unified description of different high-energy scattering experiments from deep-inelastic scattering (DIS) to complex hadronic collisions.

IP-Glasma model: A common example is the phenomenologically successful IP-Glasma model [35–38], for which the basic anatomy of the model is depicted in Fig. 2. Starting from the large scale structure, nucleons are statistically distributed inside the nucleus according to nuclear structure input, which requires the simultaneous knowledge of the fluctuating position of all nucleons in a given realization of the nucleus². Each nucleon then contains a fluctuating color charge density ρ , concentrated around N_q hot spots with a (transverse) spatial size r_H , which are statistically distributed within the size of the nucleon R_p . By virtue of Eq. (2), the color charges ρ create color fields F^{i-} , whose large distance behavior is regulated by an infrared regulator $m \sim \Lambda_{\text{QCD}}$, such that the color field of an individual charge extends over a transverse distance $\sim m^{-1}$. It is important to point out that the model also provides information on the transverse spatial structure of the field strength beyond the overall magnitude of field strength fluctuations as a function of x , which is traditionally encoded in collinear parton distribution functions. This new information

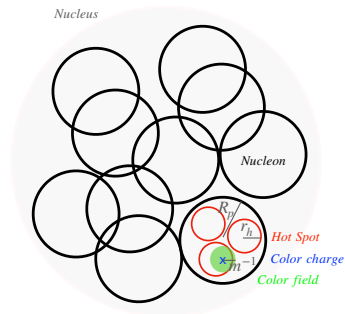


Fig. 2 Illustration of the color fields of a nucleus in an impact-parameter dependent model of the target.

²Note that the nucleon positions are assumed to remain constant over the time scale of a high-energy scattering event.

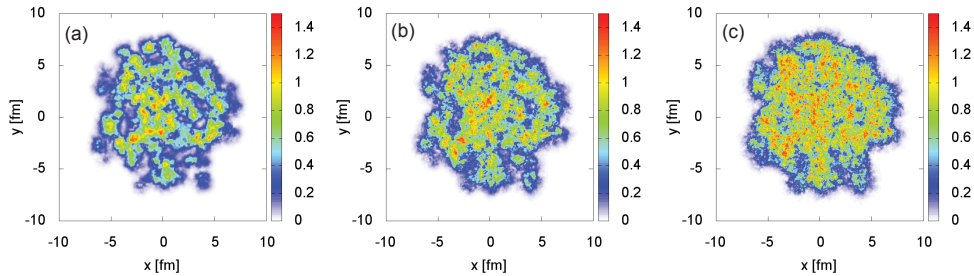


Fig. 3 Color fields of a Pb^{208} nucleus in the IP-Sat model at rapidities $x_0 \approx 2 \times 10^{-3}$, with $Y_0 = -2.4$ (left) and after $\Delta Y = 2.4$ (middle) and $\Delta Y = 4.8$ (right) units of small- x JIMWLK evolution. Figure taken from Ref. [37]

can be related to generalized parton distributions (GPDs) and transverse correlations of the field strength relevant to transverse momentum dependent (TMD) parton distributions [9, 29, 39].

The IP-Glasma model provides the magnitude of color charge fluctuations $\rho(\mathbf{x})$ at an initial scale $x_0 \sim 0.1$, such that the subsequent evolution towards smaller values of $x < x_0$ is described by the JIMWLK evolution equation [40]³. Since the model features various kinds of fluctuations, from fluctuating color charge densities at the smallest scales to nucleon positions at the largest scales, analytic calculations are usually only possible e.g. in the dilute limit [43, 44], and expectation values of observables are typically calculated by statistically sampling the averages in Eq. (7) based on a Monte Carlo procedure [45]. Each realization then provides a particular configuration of the Wilson lines $V_x(\mathbf{x})$, such that also n -point correlation functions of Wilson lines can easily be calculated [29, 46, 47], and in many cases individual realizations are interpreted as corresponding to single events (c.f. Sec. 4.2).

We illustrate this procedure in Fig. 3, which depicts a realization of the color fields of a Pb^{208} nucleus, as obtained a) at the initial scale x_0 and (b),(c) after $\Delta Y = \log(x_0/x) = 2.4, 4.8$ units of (fixed coupling) JIMWLK evolution [37]. The evolution towards smaller x is characterized by an increase of the saturation scale which is calculable perturbatively [48] and reflected by the smaller and smaller scale structures visible in Fig. 3. Beyond that the small- x evolution also inevitably leads to a growth of the transverse spatial extent of hadrons and nuclei, although the incorporation of such impact parameter dependent effects necessarily requires some additional modeling to regulate large distance emission [49–51]. In particular, this process of Gribov diffusion [52], also leads to a change of the large-scale structure of the color fields which can be seen by comparing the left and right panels of Fig. 3. While initially the color fields of the nucleus are concentrated inside the nucleons, the nucleus becomes increasingly opaque and as structure of individual nucleons is washed out towards smaller x . It would be interesting to explore, whether evidence for the predicted change of

³A variant of this is the successful IP-Sat model, where $\rho(\mathbf{x}, x)$ is provided directly as a function of x [41, 42]. More specifically, $\log \text{Tr}[V(\mathbf{b} + \mathbf{r}/2)V^\dagger(\mathbf{b} - \mathbf{r}/2)] = \frac{\pi^2}{2N_c} r^2 \alpha_S(\mu^2) \chi(\mathbf{x}, \mu^2) \Gamma(\mathbf{b})$, where the scale $\mu^2 = \mu_0^2 + C/r^2$. As the reader can see, the correlation function contains local information, probed at the average position, $|\mathbf{b}|$, while the relative direction, $|\mathbf{r}|$ sets the scale at which the target is probed.

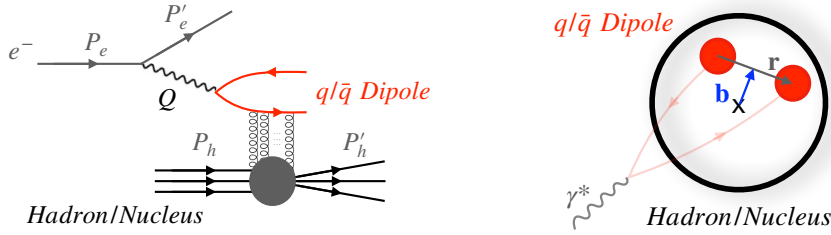


Fig. 4 Deep-Inelastic scattering (DIS) in the dipole picture.

the large scale nuclear structure can indeed be observed in very forward or very high energy scattering experiments, that probe sufficiently small values of x .

3 Probing the nuclear wavefunction: DIS

Deep-inelastic $e + p/A$ scattering experiments provide a theoretically clean way to probe the partonic structure of nucleons and nuclei. In the high-energy limit, this process is best viewed in the dipole picture [53] where, as illustrated in Fig. 4, the electron emits a virtual photon, which subsequently splits into a quark/anti-quark pair that interacts as a color dipole with the hadronic target. Due to this separation of time scales between QED and QCD processes, the leading order cross-section for the inclusive scattering of a virtual photon γ^* is given by

$$\sigma_{L,T}^{\gamma^*p}(Q^2, x) = 2 \sum_f \int \int d^2\mathbf{b} d^2\mathbf{x} \int dz \left| \Psi_{L,T}^{(f)}(r, z; Q^2) \right|^2 D(x, b, r) \quad (8)$$

The cross section is simply determined by a convolution of the QED part $\left| \Psi_{L,T}^{(f)}(r, z; Q^2) \right|^2$, representing the probability for the longitudinally (L) or transversely (T) polarized virtual photon with virtuality Q^2 to split into a q/\bar{q} dipole with momentum fractions $z, 1 - z$ and transverse separation r . The remaining ingredient is the color dipole cross-section

$$D(x, b, r) = \left\langle \frac{1}{N_c} \text{tr} [1 - V(b + r/2)V^\dagger(b - r/2)] \right\rangle_x \quad (9)$$

representing the interaction of the quark/anti-quark dipole of size r at an impact parameter b with the hadronic target [53].

Statistical comparisons to measurements of the inclusive γ^*p (reduced) cross-section at the HERA collider [54] as a function of x and Q^2 , then allow one to constrain the x and r dependence of the dipole scattering amplitude, as pioneered early on in [41, 55, 56]. However, the comparison to inclusive cross-sections suffers from the deficiency, that even at moderate values of $Q^2 \sim \text{GeV}$ it is sensitive to the contributions of non-perturbatively large dipoles ($r \gtrsim \Lambda_{\text{QCD}}^{-1}$) and does not provide information on the (transverse) geometry, associated with the impact parameter (b) dependence of

the dipole amplitude. Hence it is advantageous to consider more exclusive processes, such as e.g. the exclusive production of (heavy) vector mesons in $\gamma^* + p \rightarrow J/\psi + p$ reactions⁴, where the momentum transfer t encodes information on the impact parameter (b) dependence of the dipole amplitude [41]. Exclusive vector meson production in DIS experiments has been studied at HERA [58–61], and one distinguishes between coherent and incoherent processes, where the proton remains intact or disintegrates, which according to the Good-Walker picture [62], probe the average and fluctuations of the interaction. Experimental measurements of *coherent* vector meson production at small momentum transfer $|t| \lesssim 1\text{GeV}^2$ put a tight constraint on the average spatial extent R of the nucleon [40, 44, 55, 63]⁵, and also show intriguing hints of the energy dependence of the proton size due to small- x evolution [40, 65, 66]. Conversely, at larger momentum transfers $|t| \gtrsim 1\text{GeV}^2$, the cross-section is dominated by the *incoherent* process, the experiments also clearly demonstrate the importance of fluctuations at the subnucleonic scale, which in phenomenologically successful models is incorporated through sub-nucleonic hotspots and color charge fluctuations [43, 44], as illustrated in Fig. 2.

Similarly, to such imaging of the proton, it is also possible to probe nuclear structure at high energies, by considering deep-inelastic scattering processes off nuclear targets. While so far there is only a rather limited amount of experimental data for nuclear targets, this will change with the operation of the Electron Ion Collider (EIC), and recent works have started to develop the phenomenology of the effects of nuclear deformation and correlations of nucleons in nuclear DIS [67–69]. Beyond deep-inelastic scattering, which provides a theoretically clean probe of nuclear structure at high energies, such imaging of protons and nuclei by exclusive vector meson production can also be explored in so-called ultra-peripheral collisions (UPCs) of protons and nuclei (p+p, p+A, A+A) at RHIC and LHC, where the hadronic interaction is mediated by photon exchange [70, 71]. While the calibration of the photon flux, and the quantum interference between the photoproduction off either of the two colliding hadrons complicate the theoretical interpretation of UPCs, sophisticated techniques have recently been developed to extract $\gamma + A \rightarrow J/\Psi + A$ cross-sections from UPC measurements [72–74]. Naturally, these UPC measurements [75–81] provide access to different $\gamma + A$ center of mass energies (W), which can provide additional information on the energy dependence of nuclear and nucleon structure and the magnitude of gluon saturation effects.

3.1 New developments & open questions

New developments in the context of DIS primarily concern the quests for increasing precision and new phenomenological applications at the upcoming Electron Ion Collider (EIC) [82]. A substantial amount of effort has been dedicated to improve calculations of $e + h$ impact factors to NLO precision for observables such as DIS

⁴Similarly one could also consider the $e + p \rightarrow e + p + \gamma$ deeply virtual Compton scattering (DVCS) or $e + p \rightarrow e + p + J + J$ diffractive di-jet production processes, and we refer the interested reader to [57] (and references therein) where these processes are discussed.

⁵Since R is extracted from a process at low- x , using colored probes, this radius is to be thought of as a gluonic radius. This is in juxtaposition, for example to the charge radius of the proton as extracted from elastic scattering experiments [64]

structure functions [83–91], exclusive di-jet production [92–95] and exclusive vector meson [96, 97]. We list also recent advances in the physics of dijets/dihadron photoproduction, [98–103], semi-inclusive DIS [104–106], diffractive structure functions [107] and diffractive jets [108–110], and point to the comprehensive review provided in Ref. [111], for further information.

4 Hadronic collisions

Hadronic collisions are more complex in nature than the previous examples of DIS. The reason for this is that in hadron-hadron collisions strongly interacting degrees of freedom are present in both incoming projectiles. Because non-perturbative physics dominates at lower momenta, a general description of hadronic collisions using QCD is not available. For this purpose, we require the use of QCD Effective Field Theories (EFT) such as the CGC. In the context of the latter, particle production in hadronic collisions can be performed in two different kinematic limits, discussed separately in Sec. 4.1 and 4.2.

4.1 Forward particle production in p+p/A – the dilute-dense formalism

First, one can choose to study final states (outgoing particles) in the forward rapidity region, where outgoing states are quasi collinear to the direction of the -forward moving- incoming hadron. Because of the kinematic conditions, observables in the forward region are dominated by large- x degrees of freedom in the forward moving hadron, such that collinear factorization is applicable to it. Consequently, particle production in the forward region can be viewed as a process where single partons in the projectile can scatter off the color fields of the backward moving hadron, which is then usually referred to as the target. When the center-of-mass energy is sufficiently high, the target is dominated by small- x gluons requiring a dedicated treatment of multiple parton interactions. Stated differently, this means that in forward kinematics, one is using a single parton coming from a *dilute* projectile to probe the complex small- x wavefunction of a *dense* hadronic target.

Summarizing the above discussion, collinear factorization applies in the dilute projectile, while in the dense target, it is not applicable as interaction with small- x partons need to be taken into account to all orders, just as in the last section. Generally, forward scattering processes can thus be viewed as $p_i + A \rightarrow p_1 + \dots + p_n + X$ reactions, where a single perturbative parton p_i from the projectile, exhibits multiple-scattering from the target A , producing outgoing partons $p_1 \dots p_n$, resulting from splittings, radiation off the first incoming parton. This semi-perturbative way of computing cross-sections is commonly called the dilute-dense or hybrid formalism in the literature [112–114].

Clearly, the simplest process one can focus on is single inclusive hadron production in the forward dilute-dense limit, for which the leading order cross-section is given by [112, 115]

$$\frac{d\sigma^{pA \rightarrow hX}}{dy d^2\mathbf{k}_T d^2\mathbf{b}} = \int dx dz \frac{1}{z^2} q(x, Q_f^2) \frac{d\sigma_{qA}^{tot}}{dy_q d^2\mathbf{q}_T d^2\mathbf{b}} D_{q/h}(z, Q_f^2) \quad (10)$$

where we assumed for simplicity that the interacting parton in the projectile is an incoming quark⁶. The momentum of the produced hadron is related to the momentum of the parton via $\mathbf{k}_T = z\mathbf{q}_T$. This formula exemplifies perfectly the three ingredients needed for any forward computation. Starting from the partonic content of the projectile, determined by the non-perturbative collinear quark distribution $q(x, Q_f^2)$, the factor σ_{qA}^{tot} represents the cross-section for the interaction of the incoming quark with the target, namely $q_i + A \rightarrow q_f + X$, in our notation above. Eventually, the scattered quark undergoes a fragmentation process to produce the final state hadron, as described by the non-perturbative fragmentation function $D_{q/h}(z, Q_f^2)$. By following the discussion in Sec. 2, the cross-section for the interaction of the incoming quark with the target can be computed in the Color Glass Condensate framework as

$$\frac{d\sigma_{qA}^{tot}}{dy_q d^2\mathbf{q} d^2\mathbf{b}} = \frac{1}{(2\pi)^2} \tilde{S}(x, \mathbf{q}, \mathbf{b}) \quad (11)$$

where $\tilde{S}(x, \mathbf{q}_T, \mathbf{b}) = 1 - \tilde{D}(x, \mathbf{q}_T, \mathbf{b})$ is the Fourier transform of the dipole operator in the fundamental representation [115].

Similarly, to the above example of single inclusive hadron production, the hybrid formalism can be applied to more complex forward observables, such as single and multiple jets [112, 116–120] (and references therein), or electromagnetic probes [121–125]. Generally, the anatomy of the relevant cross-sections remains identical, as the underlying partonic cross-section is calculated within the CGC framework, while the distribution of incoming partons in the projectile is determined by collinear parton distribution functions, just as in perturbative QCD. When considering hadronic observables, one also needs the knowledge of how the outgoing partons hadronize, which is usually obtained by convolving the cross-section with fragmentation functions $D_{q/h}(z, Q_f^2)$, which are non-perturbative functions extracted from experiment [126]. Evidently, in the case of multi-parton outgoing states, the convolution with fragmentation functions is needed for each of the outgoing states, as would e.g. be the case for the NLO correction for a quark scattering off a gluonic target, $q + A \rightarrow q + g + X$, where one needs to convolve the cross-section with both $q \rightarrow h$ and $g \rightarrow h$ fragmentation functions if one is interested in the hadronic end-states.

4.1.1 *Status Quo*: forward p+A collisions

As it was mentioned above, the main physical point of choosing final states (outgoing particles) aligned around the forward rapidity region is to enhance the access to the saturated degrees of freedom in the target. As the collinear charges move through the cold nuclear matter (CNM⁷) they scatter multiple times from the gluons in the target, modifying the spectra of the charges after the interaction.

⁶Note that a similar expression as in Eq. (10) can be obtained for any forward parton interacting with the dense hadronic target. Nevertheless, in the very forward limit, where the cross-section is dominated by large- x partons in the dilute projectile, collinear quarks will dominate over collinear gluons. We will see later that gluons become more relevant in the context of di-jet production.

⁷This is a name used in the literature to call the nuclear effects of the complex nuclear target. It refers to the view of this incoming nucleus as a small, cold "medium" of nuclear matter. The term cold is used in contra-position to the *hot* nuclear medium, the QGP.

In $p + A$ collisions, the first step is to explore spectra of (un-)identified particles. A useful tool to extract information about the saturation effects of the nucleus in such systems is the so-called nuclear modification factor R_{pA} ,

$$R_{pA} = \frac{d\sigma_{pA}/dp_T dy}{N_{\text{coll}} d\sigma_{pp}/dp_T dy} \quad (12)$$

where particle production in $p + A$ collisions is compared to pp , scaled by the number of binary collisions, N_{coll} . The R_{pA} has been measured using different nuclear targets (see, e.g. Refs. [127, 128]) where a reduction of the total emission ($R_{pA} < 1$) was seen for hadrons along the p-going direction. This is consistent with the physical picture of the CGC, where the multiple-scattering of the forward projectile with the coherent target is expected to cause reduction of particle emission at lower p_T [25], causing a flatter spectrum in comparison to the perturbative $dN/dp_T dy \sim p_T^{-4}$. Much more sensitive signals than single particle spectra are particle correlations [47, 116, 129–132]. In this case, one can look at the correlations of two forward independent hadrons, $p(p_p) + A(p_A) \rightarrow h_1(p_1) + h_2(p_2) + X$, or at the production of two forward jets, $p(p_p) + A(p_A) \rightarrow j_1(p_1) + j_2(p_2) + X$, see for example Fig. 5. While the measured object itself is not the same⁸, both present the same initial mechanism, namely the particle production through radiation or splitting from the incoming forward parton.

The initial parton restricts, through the initial hard scatterings/splittings, the nature of the initial partons for the jets (j_1 and j_2). On the other hand, multiple scatterings with the soft gluons within the target determine the transverse momentum imbalance between the two jets, $\mathbf{q}_T = \mathbf{p}_{1,T} - \mathbf{p}_{2,T}$. The crux of this point is that, as $|q_T|$ approaches the saturation scale of the target, the dijet correlation becomes sensitive to saturation effects in the gluon distributions. Intuitively, the partonic pair has the "relative size" large enough to multiply interact with a highly occupied set of gluons. The first effect of this is that the transverse momentum broadening caused by such interactions causes the suppression of the correlation at small relative momenta. Additionally, the deflection of the pair causes a broadening of the angular distribution of the two particles, where the back-to-back peak (at $\Delta\phi = \pi$) becomes softer and broadened. In Fig. 6, taken from Ref. [133], the reader can find the saturation

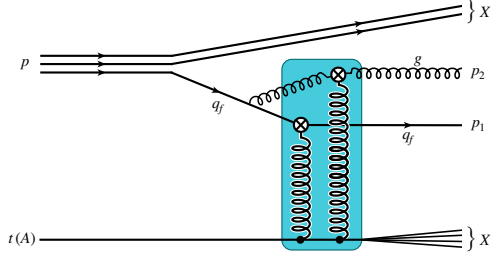


Fig. 5 Kinematics of dijet production for the dilute-dense case, in the case of forward qg dijets. Here a quark q_f of the proton emits a gluon g and both interact with the incoming target (t). Through the interaction the quark and the gluon acquire with momenta p_1 and p_2 , respectively.

⁸In the case of hadrons, the partonic cross-section needs to be convoluted with the fragmentation functions of the outgoing partons, just as in eq. (10). For jet production, the parton needs to be evolved by radiating/splitting towards lower momenta, effectively creating a parton *cascade*, or *shower*, which in general will be more sensitive to final state effects.

effects as visible in the nuclear modification factor for forward dijet production, as computed in the improved TMD factorization formalism [30], which, loosely speaking, corresponds to the $|\mathbf{p}_{1/2,T}| \gg Q_s$ limit of the CGC EFT [134, 135]. In the left plot, the reader can see an overall suppression of the jet production, which becomes stronger with decreasing transverse momentum p_T^1 of the leading jet. On the right side, we also have a nuclear modification factor, but now for angular distributions. One can read from this image the aforementioned effect of the suppression of back-to-back correlations. This effect, predicted in Ref. [129], was later experimentally found at RHIC by the PHENIX collaboration [136, 137]. Additionally, LHC has measured dijet yields at forward rapidities in proton-proton and proton-lead collisions, although the search for saturation signals in these observables was not conclusive enough [138].

A particularly powerful tool to explore the gluon wave-functions of the initial state are electromagnetic probes, photons and dileptons. Devoid of strong interactions, the EM probes created by interactions with the saturated target are themselves the final states observed. Measurements of forward isolated photons have been collected by the ATLAS and CMS collaborations for moderate rapidities in proton-proton collisions and for intermediate transverse momentum [139–142]. Photon (dilepton) production has been computed for dilute dense system at LO in Ref. [121, 122]. The extension to NLO -in the CGC power counting scheme- has been performed in Refs. [123, 124, 143, 144]⁹. Because of the kinematics of gluon fusion, the NLO is more relevant at lower rapidities, the overlap regions at intermediate rapidities are an interesting case to explore the sensitivity to the gluon distributions in the projectile. Just as in the dihadron case, photon-hadron correlations are more sensitive to saturation physics [125].

4.1.2 New developments & open questions

While the most promising phenomenological signatures of small- x gluon saturation remain the same, over the last decade, the field has worked towards achieving higher-order precision, which involves developing concurrent corrections both to the individual cross-sections and to the x -evolution of the gluon distributions. A significant amount of progress has been achieved to describe hadronic collisions in the dilute-dilute and dilute dense to NLO accuracy on the side of the impact factors, both on single particle production formulas [117, 118, 148, 149] and for dijet production in pA [120]. Early works famously saw negative cross-sections at large- p_T [148–150], a problem which has received two independent solutions [151, 152]. The reader can find a phenomenological analysis using the solution [152] in Ref. [153]. On the other hand, quite some effort has gone to improve the small- x evolution equations from the well established leading logarithm (LL) level –including running coupling effects – to the NLL accuracy, effects which have been derived for the BK [154] and JIMWLK equations [155–159]. Additionally, NLL corrections to the JIMWLK evolution have been recently derived also for massive quark corrections in Ref. [160]. It is important to note also that the numerical implementation of these equations has proven to be a

⁹While NLO parton emission has been computed in Refs.[145, 146] for the equivalent mechanism in DIS, NLO emission is still not fully understood in the dilute-dense limit of the CGC. However, NLO corrections to LO channel have been performed in the TMD factorization limit by including gluon emission[147]

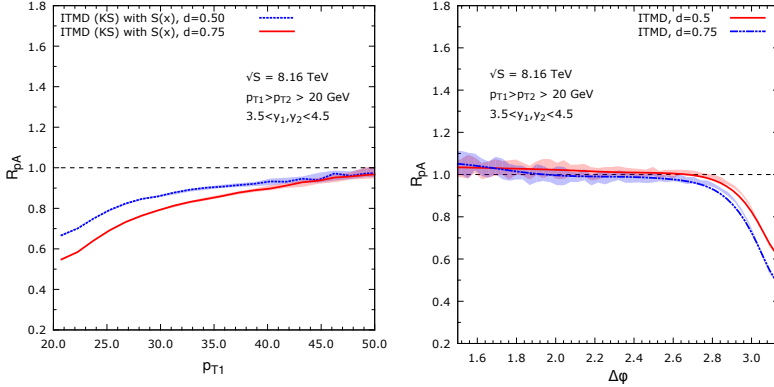


Fig. 6 (Left) Nuclear modification factors as a function of the transverse momentum of the leading jet. (Right) Nuclear modification factors of the angular distribution for two jets, shown for two values of the nuclear saturation scale. At large angles, the p+A dijet angular distribution sees an effective suppression. Here, the parameter d estimates the uncertainty in the strength of saturation in Pb nuclei (as deviation from $Q_A^2 \sim A^{2/3} Q_p^2$). Figures taken from Ref. [133].

complex task, where e.g. numerical instabilities on the solution of NLL BK equations were found for phenomenologically relevant initial conditions, and later fixed by additional resummations [161–163]. Obtaining full numerical evolution of the JIMWLK equation at NLL is still an active area of research [164].

So far a sophisticated modeling of nuclear geometry and multiplicity dependent effects has not been performed for many dilute-dense CGC calculations. However, it has recently been shown in Ref. [47], that nuclear structure modeling in the gluon distributions leadseems to a dependenc have an effect on the saturation scale different from thean naively expected from $Q_s^2 \sim A^{1/3}$, altering the naive expectations (and computations) based on such behavior. Since forward particle production provides a natural way of constraining our knowledge of the initial small- x many-body wavefunction of the colliding hadrons, improvements in this respect would be also desirable in order to reduce theoretical uncertainties in the initial deposition of charge and energy in heavy-ion collisions (see Sec. 4.2) and improve the predictive power of the entire framework.

4.2 Initial state of Heavy-Ion Collisions (HICs) – the dense-dense formalism

High-energy heavy-ion collisions produce a complex QCD many-body system, whose space-time evolution is conventionally described within multi-stage evolution models [165], including the energy deposition and early-time dynamics in the initial state, the viscous hydrodynamic evolution of the Quark-Gluon Plasma (QGP), the re-hadronization of the QGP as well as the subsequent re-scattering and decay of produced hadrons. In this context the CGC framework provides a QCD approach to compute the properties of the initial state, from the underlying structure of hadrons and nuclei. Stated differently, due to the complex reaction dynamics, the scope of

CGC calculations is not to describe the final state particle spectra observed in heavy-ion collisions, but merely to obtain the space-time structure of the initial state shortly after the collision, which in turn can then be used as a starting point for describing the subsequent reaction dynamics.

In high-energy collisions kinematics dictates that the energy deposition around mid-rapidity is dominated by small- x gluons, which are highly abundant in the colliding nuclei. Both nuclei are then typically considered as "dense" color charged objects, and described in terms of counter-propagating eikonal color currents [3]

$$J_{A/B}^\mu = \delta^{\mu\pm} \delta(x^\mp) t^a \rho_{A/B}^a(\mathbf{x}_T). \quad (13)$$

localized around the $x^\pm = 0$ axis, where the subscript A/B refers to the two incoming nuclei moving along the positive/negative $\pm z$ direction. In order to describe the ensuing dynamics we will use Milne coordinates,

$$x^\pm = \frac{\tau}{\sqrt{2}} e^{\pm\eta_s} \quad \Rightarrow \quad \tau = \sqrt{2x^+x^-}, \quad \eta_s = \frac{1}{2} \log \left[\frac{x^+}{x^-} \right], \quad (14)$$

where τ is the longitudinal proper time and η_s is the space-time rapidity. We also note in passing that in terms of the Milne coordinates, the fields are now given by

$$\tau A^\tau = x^+ A^- + x^- A^+ \quad \text{and} \quad \tau^2 A^{\eta_s} = x^+ A^- - x^- A^+ \quad (15)$$

while the transverse components A^i are unaffected by the transformation.

Developing a first principles description of the real-time non-equilibrium dynamics of QCD is an outstanding problem [166]. However, at leading order in the strong coupling constant the ensuing dynamics of the collision are described by the solution to the classical Yang-Mills (CYM) equations [167]

$$D_\mu F^{\mu\nu} = J^\nu \quad (16)$$

where in Fock-Schwinger ($A^\tau = 0$) gauge, the eikonal color currents are individually conserved ($D_\mu J_{A/B}^\mu = 0$), such that $J^\mu = J_A^\mu + J_B^\mu$ denotes the combined color current of both colliding nuclei¹⁰. Next-to-leading order corrections include quantum fluctuations on top of the CYM equations [35, 173–175], however a consistent NLO description is yet to be developed.

The solution to Eq. (16) can be conveniently expressed by subdividing space-time in four regions

$$A^\mu(x) = \theta(-x^-)\theta(-x^+) A_0^\mu(x) + \theta(x^-)\theta(-x^+) A_A^\mu(x) \\ + \theta(-x^-)\theta(x^+) A_B^\mu(x) + \theta(x^-)\theta(x^+) A_{AB}^\mu(x) \quad (17)$$

depending on whether or not causal contact with nucleus A and B has been established, as illustrated in Fig. 7. Starting from the classical vacuum $A_0^\mu(x) = 0$ before

¹⁰If this is not the case, the covariant conservation equation $D_\mu J^\mu = 0$ needs to be solved concurrently with the class. Yang-Mills equations, with boundary conditions describing the incoming nuclei prior to the collision (see e.g. [168–172]).

the collision, the solutions in regions A and B are the same as in the case of a single nucleus, such that the field strength $F^{\mp i}$ is located inside the nuclei at $x^\pm \simeq 0$, and the non-vanishing components of the gauge field in Fock-Schwinger gauge are given by

$$A_A^i(x) = \frac{i}{g} V_A^\dagger(x) \partial^i V_A(x) \quad \text{and} \quad A_B^i(x) = \frac{i}{g} V_B^\dagger(x) \partial^i V_B(x). \quad (18)$$

where $V(x)$ denote the light-like Wilson lines as in Eq. (5).¹¹ Due to the non-linear nature of the CYM equations, analytical solutions are no longer available for the evolution in the forward light-cone(AB). Strikingly, however, the initial conditions for the evolution in the forward light-cone (AB), at $\tau = 0^+$, immediately after the collision, can still be determined in a closed form [176, 177],

$$\begin{aligned} A^{\eta s}(\tau \rightarrow 0^+, \eta^s, \mathbf{x}_T) &= \frac{ig}{2} [A_A^i(\mathbf{x}_T), A_B^i(\mathbf{x}_T)] \\ A^i(\tau \rightarrow 0^+, \eta^s, \mathbf{x}_T) &= A_A^i(\mathbf{x}_T) + A_B^i(\mathbf{x}_T) \end{aligned} \quad (19)$$

which represent boost-invariant longitudinal chromo-electric and chromo-magnetic fields, mediating the color exchange between the colliding nuclei [178]. Since the τ -derivatives of the fields can be found to vanish at $\tau \rightarrow 0$, the source-free classical Yang-Mills (CYM) equations (16), along with the gauge fields in Eq. (19) represent an initial value problem for the space-time evolution in region (AB).

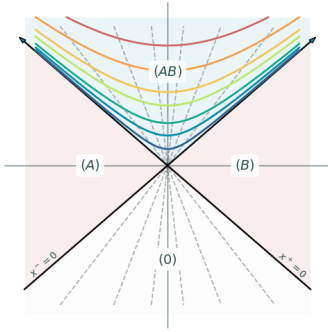


Fig. 7 Space-time diagram for the evolution of a high-energy heavy-ion collisions

Starting from the initial “Glasma” fields in Eq. (19), different aspects of the subsequent space-time dynamics can be studied (semi-) analytically based on perturbative [46] or proper time expansions [179, 180], or numerically using real-time lattice gauge theory techniques to solve the CYM equations in the forward light-cone [181–183]. By consistently following the perturbative approach, one recovers factorization formulas for inclusive particle production in the dilute limit [46, 184], which provide the basis for the MCDIPPER initial state model of heavy-ion collisions [31]. Numerical simulations of the CYM equations underlie the phenomenologically successful IP-Glasma model [35, 36], which employs the color charge configurations of the IP-Sat model described in Sec. 2, to compute the energy-momentum tensor of the Glasma,

$$T^{\mu\nu} = -F^{\mu\rho} F_\rho^\nu + \frac{1}{2} g^{\mu\nu} F_{\lambda\sigma} F^{\lambda\sigma}. \quad (20)$$

¹¹Evidently, the solution in Fock-Schwinger (FS) gauge can be directly obtained from the individual solutions (2) in light-cone (LC) gauge, by performing a gauge transformation $A_{FS}^\mu(x) = G^\dagger(x) A^\mu(x) G(x) + \frac{i}{g} G^\dagger(x) \partial^\mu G(x)$ with $G(x) = \mathcal{P} \exp(\int_{-\infty}^x dz^+ ig A^-(x^+, x_T)) \mathcal{P} \exp(\int_{-\infty}^x dz^- ig A^+(x^-, x_T))$.

Initially the longitudinal chromo-electric and chromo-magnetic Glasma flux tubes give rise to the following diagonal form of the energy-momentum tensor

$$T_{\nu}^{\mu}(\tau = 0^+) |_{\text{Glasma}} = \text{diag}(e_0, e_0, e_0, -e_0) \quad (21)$$

which describes a non-equilibrium system in its rest frame, with local energy density $e_0(x) = T_{\tau}^{\tau}(x)$ and negative longitudinal pressure $\tau^2 T^{\eta\eta} = -e_0(x)$. However, on a time scale $\tau \sim 1/Q_s$ phase decoherence of the classical fields rapidly leads to a different form of the energy-momentum tensor

$$T_{\nu}^{\mu}(\tau_{\text{EKT}} = 1/Q_s) |_{\text{EKT}} \simeq \text{diag}(e, e/2, e/2, 0) \quad (22)$$

which describes a system of weakly interacting quasi-particles, with transverse momenta $\sim Q_s$ and vanishing longitudinal momenta in the local rest frame u^{μ} , which neglecting the off-diagonal components of $T^{\mu\nu}$, related to transverse expansion (pre-flow), is given by $u^{\mu} = (1, 0, 0, 0)$ in Milne coordinates. Despite the fact that at this point the system is still highly anisotropic, the initial state in Eq. (22) is successfully used as initial conditions for the subsequent hydrodynamic evolution of the QGP [185]. In this case, the system is still far from equilibrium at the beginning of the hydrodynamics phase, and the evolution towards equilibrium is then described macroscopically by *viscous* hydrodynamics. Since at $\tau \sim 1/Q_s$, the system can be described by weakly interacting quasi-particles, one alternative is to describe its evolution towards equilibrium using QCD kinetic theory [186–188], which naturally leads to a near-equilibrium form of the energy momentum tensor

$$T_{\nu}^{\mu}(\tau = \tau_{\text{th}}) |_{\text{Hydro}} = \text{diag}(e, e/3, e/3, e/3) + \text{viscous corrections.} \quad (23)$$

and also describes the evolution of pre-equilibrium flow. Evidently, understanding the microscopic mechanisms behind equilibrium and the onset of hydrodynamic behavior is one of the most outstanding challenges in contemporary heavy-ion physics, and we refer to [166, 189] for dedicated reviews on this subject. Nevertheless, it is important to properly describe the pre-equilibrium stage, as the duration of the pre-equilibrium stage determines the overall amount of energy deposition and also has a non-trivial impact on the collision geometry [190]. Since the CGC initial state models are based on microscopic QFT calculations, they also give access to momentum space information and the possibility to include initial state momentum correlations [191]. However, such correlations will then be destroyed by subsequent space-time evolution of the QGP [192, 193], they are relatively short range in rapidity [194] and decrease with increasing system size [51, 195] and may thus only be relevant in short-lived small collision systems.

Generally, initial state models based on saturation physics provide not only the spatial geometry, but also the overall magnitude and center-of-mass energy dependence of energy deposition in the initial state of heavy-ion collisions. Beyond the concrete implementations of these ideas in the IP-Glasma [35]¹², the MCDIPPER [31]¹³, as well

¹²Based on the IP-Sat model and real-time lattice gauge theory simulations of the CYM equations.

¹³Based on the IP-Sat model and a k_T -factorized approximation to the CYM equations.

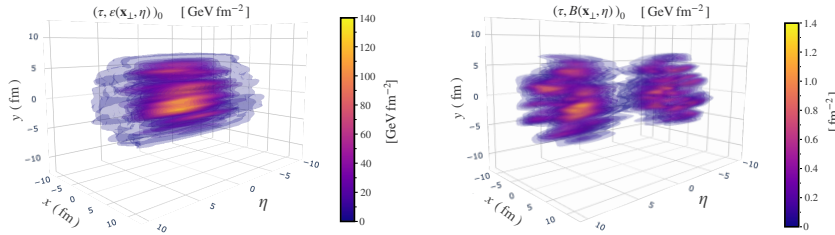


Fig. 8 Deposition of energy density (*left*) and baryon charge (*right*) for a single 3D event. The charge and energy deposition is computed in the initial state MCDIPPER framework. Figure taken from Ref. [209].

as the saturation inspired EKRT model [196, 197]¹⁴, the insights from such microscopic calculations have also proven valuable for the development of empirical initial state models. Such is the case of TrENTo [198], where energy and charge deposition in heavy-ion collisions are determined according to relatively simple parametric formulas. Notably, a detailed statistical analysis of heavy-ion data seems to support the general dependence inferred from saturation models [199]. Since the CGC models are independently constrained from DIS experiments, the initial state of heavy-ion collisions is actually reasonably well constrained, meaning that comparisons to experimental heavy-ion data should provide rather stringent constraints on the space-time evolution of the QGP, that connects the initial state to experimental measurements. However in practice this potential has not been fully exploited, as it is common practice in heavy-ion phenomenology to re-adjust e.g. the normalization of the initial state energy, in order to reproduce measured particle spectra.

It is also important to note that since the models are based on QCD structure of nucleons, they are not limited to heavy-ion collisions but in principle applicable to collisions of all hadronic species at sufficiently high center of mass energy. In particular for small systems, effects of sub-nucleonic structure resulting in a non-trivial proton geometry, are in fact essential for the description of collective flow in p+A collision [200], albeit it is not clear to what extent a hydrodynamic description of the space-time evolution is quantitatively accurate in small systems [201]. Conversely, in large collision systems, such as A+A collisions - with Au, Pb nuclei - the relevant aspects of geometry are determined by fluctuations at the largest scales, namely the nucleon positions. Since in this case, the most relevant fluctuations are set at distances of 1-10 fm, correlations of low-energy nuclear structure start becoming important, and there are ongoing efforts to explore effects of α -clustering [202, 203], ground state deformation [204–206] and the appearance of a neutron skin [207, 208] for different nuclear species.

4.2.1 New developments & open questions

Currently one of the most important challenges in describing the initial state of heavy-ion collisions, is the development of a first principles understanding of the $3+1D$ space-time structure of the initial state. Generally, the CGC provides a natural framework to

¹⁴Based on collinear factorization with final state saturation imposed.

address this question, however so far it has proven challenging to develop a consistent formulation of the 3+1D dense-dense collisions.

By extending the support of the eikonal color currents in Eq. (13) to a finite longitudinal thickness, different implementations of a 3+1 D coordinate space picture of the Glasma have been put forward [168, 169, 172, 210–213]. However, it is not yet clear how to fully relate the longitudinal structure of the eikonal color currents to the small x structure of the colliding nuclei. While this relation should partially come from the JIMWLK evolution, other aspects, e.g. the sources finite size [168, 172], may have an important impact. Additionally, it remains to be seen how genuine sub-eikonal corrections [214, 215] could be incorporated into this framework.

Phenomenological saturation models for the 3+1D initial state of heavy-ion collisions, instead employ a momentum space picture, which emerges in the dilute-dense limit, where it becomes possible to establish a relationship between the momentum fractions x of incoming partons and the momentum rapidity y of produced partons [31, 216–218]. One example is the MCDIPPER model [31, 219], which is phrased in the language of TMDs, where e.g. the initial charge deposition due to valence quark stopping is determined by the probability of the valence charge acquiring transverse momentum from the interaction with saturated gluons in the target (see [220])¹⁵.

Notably in the momentum space picture, it is in principle straightforward to include the energy and charge deposition due to quarks, as done e.g. in the MCDIPPER, as well as higher order perturbative corrections, albeit this has not been accomplished to date. By identifying space-time and momentum rapidity one then obtains a coordinate space picture of the 3D initial state, as illustrated in Fig. 8.

We finally note that beyond the development of concrete implementations, there are more fundamental questions regarding the validity of factorization assumptions when considering un-equal rapidity correlations [221], which will require further attention in the future.

5 Concluding Remarks

Effective theories for high-energy nuclear interactions, provide important insights into the behavior of nuclear matter under extreme conditions. By modeling the complex gluon dynamics at small- x , the Color Glass Condensate (CGC) framework represents a significant step towards a unified description of high-energy scattering processes in QCD, bridging experimental observations in lepton-hadron, hadron-hadron and hadron-nucleus collisions with theoretical models. While leading order cross-section calculations in the CGC provide an intuitive understanding of the underlying physics picture, phenomenological studies based on higher order calculations will be key in refining our understanding of QCD at high CoM energies and enhancing predictive capabilities for both current and next-generation colliders. Beyond the precision frontier, new developments, especially those addressing longitudinal correlations and the three-dimensional many-body structure of hadrons, will be instrumental for the development of a cohesive physical picture of nuclei at high energies. Even though it is

¹⁵By expanding in the transverse momentum transfer from the target to the projectile is, one can recover the collinear factorization limit, in which models such as EKRT also provide a 3D picture of the initial state [197].

presently unclear when or to what extent a smoking gun signal for gluon saturation at small x will be discovered at present or future facilities, it is clear that the general theoretical framework of saturation physics will continue to provide important contributions to unraveling the fundamental structure of nuclear matter at extreme scales.

Acknowledgments. We thank B. Schenke and the referees of EPJA for excellent comments and suggestions. The authors acknowledge support by the Deutsche Forschungsgemeinschaft (DFG, German Research Foundation) through the CRC-TR 211 ‘Strong-interaction matter under extreme conditions’-project number 315477589 – TRR 211.

References

- [1] Gelis, F., Iancu, E., Jalilian-Marian, J., Venugopalan, R.: The Color Glass Condensate. *Ann. Rev. Nucl. Part. Sci.* **60**, 463–489 (2010) <https://doi.org/10.1146/annurev.nucl.010909.083629> [arXiv:1002.0333](https://arxiv.org/abs/1002.0333) [hep-ph]
- [2] McLerran, L.D., Venugopalan, R.: Computing quark and gluon distribution functions for very large nuclei. *Phys. Rev. D* **49**, 2233–2241 (1994) <https://doi.org/10.1103/PhysRevD.49.2233> [arXiv:hep-ph/9309289](https://arxiv.org/abs/hep-ph/9309289)
- [3] McLerran, L.D., Venugopalan, R.: Gluon distribution functions for very large nuclei at small transverse momentum. *Phys. Rev. D* **49**, 3352–3355 (1994) <https://doi.org/10.1103/PhysRevD.49.3352> [arXiv:hep-ph/9311205](https://arxiv.org/abs/hep-ph/9311205)
- [4] McLerran, L.D., Venugopalan, R.: Fock space distributions, structure functions, higher twists and small x . *Phys. Rev. D* **59**, 094002 (1999) <https://doi.org/10.1103/PhysRevD.59.094002> [arXiv:hep-ph/9809427](https://arxiv.org/abs/hep-ph/9809427)
- [5] Ethier, J.J., Nocera, E.R.: Parton Distributions in Nucleons and Nuclei. *Ann. Rev. Nucl. Part. Sci.* **70**, 43–76 (2020) <https://doi.org/10.1146/annurev-nucl-011720-042725> [arXiv:2001.07722](https://arxiv.org/abs/2001.07722) [hep-ph]
- [6] Diehl, M.: Introduction to GPDs and TMDs. *Eur. Phys. J. A* **52**(6), 149 (2016) <https://doi.org/10.1140/epja/i2016-16149-3> [arXiv:1512.01328](https://arxiv.org/abs/1512.01328) [hep-ph]
- [7] Ji, X.: Generalized parton distributions. *Ann. Rev. Nucl. Part. Sci.* **54**, 413–450 (2004) <https://doi.org/10.1146/annurev.nucl.54.070103.181302>
- [8] Boussarie, R., et al.: TMD Handbook (2023) [arXiv:2304.03302](https://arxiv.org/abs/2304.03302) [hep-ph]
- [9] Diehl, M.: Generalized parton distributions. *Phys. Rept.* **388**, 41–277 (2003) <https://doi.org/10.1016/j.physrep.2003.08.002> [arXiv:hep-ph/0307382](https://arxiv.org/abs/hep-ph/0307382)
- [10] Belitsky, A.V., Ji, X.-d., Yuan, F.: Quark imaging in the proton via quantum phase space distributions. *Phys. Rev. D* **69**, 074014 (2004) <https://doi.org/10.1103/PhysRevD.69.074014> [arXiv:hep-ph/0307383](https://arxiv.org/abs/hep-ph/0307383)

- [11] Klasen, M., Paukkunen, H.: Nuclear PDFs After the First Decade of LHC Data (2023) <https://doi.org/10.1146/annurev-nucl-102122-022747> arXiv:2311.00450 [hep-ph]
- [12] Cichy, K., Constantinou, M.: A guide to light-cone PDFs from Lattice QCD: an overview of approaches, techniques and results. *Adv. High Energy Phys.* **2019**, 3036904 (2019) <https://doi.org/10.1155/2019/3036904> arXiv:1811.07248 [hep-lat]
- [13] Kuraev, E.A., Lipatov, L.N., Fadin, V.S.: Multi - Reggeon Processes in the Yang-Mills Theory. *Sov. Phys. JETP* **44**, 443–450 (1976)
- [14] Kuraev, E.A., Lipatov, L.N., Fadin, V.S.: The Pomeranchuk Singularity in Nonabelian Gauge Theories. *Sov. Phys. JETP* **45**, 199–204 (1977)
- [15] Balitsky, I.I., Lipatov, L.N.: The Pomeranchuk Singularity in Quantum Chromodynamics. *Sov. J. Nucl. Phys.* **28**, 822–829 (1978)
- [16] Balitsky, I.: Operator expansion for high-energy scattering. *Nucl. Phys. B* **463**, 99–160 (1996) [https://doi.org/10.1016/0550-3213\(95\)00638-9](https://doi.org/10.1016/0550-3213(95)00638-9) arXiv:hep-ph/9509348
- [17] Kovchegov, Y.V.: Small x $F(2)$ structure function of a nucleus including multiple pomeron exchanges. *Phys. Rev. D* **60**, 034008 (1999) <https://doi.org/10.1103/PhysRevD.60.034008> arXiv:hep-ph/9901281
- [18] Iancu, E., Leonidov, A., McLerran, L.D.: The Renormalization group equation for the color glass condensate. *Phys. Lett. B* **510**, 133–144 (2001) [https://doi.org/10.1016/S0370-2693\(01\)00524-X](https://doi.org/10.1016/S0370-2693(01)00524-X) arXiv:hep-ph/0102009
- [19] Iancu, E., Leonidov, A., McLerran, L.D.: Nonlinear gluon evolution in the color glass condensate. 1. *Nucl. Phys. A* **692**, 583–645 (2001) [https://doi.org/10.1016/S0375-9474\(01\)00642-X](https://doi.org/10.1016/S0375-9474(01)00642-X) arXiv:hep-ph/0011241
- [20] Iancu, E., McLerran, L.D.: Saturation and universality in QCD at small x . *Phys. Lett. B* **510**, 145–154 (2001) [https://doi.org/10.1016/S0370-2693\(01\)00526-3](https://doi.org/10.1016/S0370-2693(01)00526-3) arXiv:hep-ph/0103032
- [21] Mueller, A.H.: A Simple derivation of the JIMWLK equation. *Phys. Lett. B* **523**, 243–248 (2001) [https://doi.org/10.1016/S0370-2693\(01\)01343-0](https://doi.org/10.1016/S0370-2693(01)01343-0) arXiv:hep-ph/0110169
- [22] Rummukainen, K., Weigert, H.: Universal features of JIMWLK and BK evolution at small x . *Nucl. Phys. A* **739**, 183–226 (2004) <https://doi.org/10.1016/j.nuclphysa.2004.03.219> arXiv:hep-ph/0309306
- [23] Golec-Biernat, K.J., Wusthoff, M.: Saturation effects in deep inelastic scattering

- at low Q^{*2} and its implications on diffraction. *Phys. Rev. D* **59**, 014017 (1998) <https://doi.org/10.1103/PhysRevD.59.014017> arXiv:hep-ph/9807513
- [24] Bjorken, J.D.: Asymptotic Sum Rules at Infinite Momentum. *Phys. Rev.* **179**, 1547–1553 (1969) <https://doi.org/10.1103/PhysRev.179.1547>
- [25] McLerran, L.D.: The Color glass condensate and small x physics: Four lectures. *Lect. Notes Phys.* **583**, 291–334 (2002) https://doi.org/10.1007/3-540-45792-5_8 arXiv:hep-ph/0104285
- [26] Dumitru, A., Skokov, V., Ullrich, T.: Measuring the Weizsäcker-Williams distribution of linearly polarized gluons at an electron-ion collider through dijet azimuthal asymmetries. *Phys. Rev. C* **99**(1), 015204 (2019) <https://doi.org/10.1103/PhysRevC.99.015204> arXiv:1809.02615 [hep-ph]
- [27] Petreska, E.: TMD gluon distributions at small x in the CGC theory. *Int. J. Mod. Phys. E* **27**(05), 1830003 (2018) <https://doi.org/10.1142/S0218301318300035> arXiv:1804.04981 [hep-ph]
- [28] Mulders, P.J., Rodrigues, J.: Transverse momentum dependence in gluon distribution and fragmentation functions. *Phys. Rev. D* **63**, 094021 (2001) <https://doi.org/10.1103/PhysRevD.63.094021> arXiv:hep-ph/0009343
- [29] Marquet, C., Petreska, E., Roiesnel, C.: Transverse-momentum-dependent gluon distributions from JIMWLK evolution. *JHEP* **10**, 065 (2016) [https://doi.org/10.1007/JHEP10\(2016\)065](https://doi.org/10.1007/JHEP10(2016)065) arXiv:1608.02577 [hep-ph]
- [30] Kotko, P., Kutak, K., Marquet, C., Petreska, E., Sapeta, S., Hameren, A.: Improved TMD factorization for forward dijet production in dilute-dense hadronic collisions. *JHEP* **09**, 106 (2015) [https://doi.org/10.1007/JHEP09\(2015\)106](https://doi.org/10.1007/JHEP09(2015)106) arXiv:1503.03421 [hep-ph]
- [31] Garcia-Montero, O., Elfner, H., Schlichting, S.: The McDIPPER: A novel saturation-based 3+1D initial state model for Heavy Ion Collisions (2023) arXiv:2308.11713 [hep-ph]
- [32] Jalilian-Marian, J., Kovner, A., McLerran, L.D., Weigert, H.: The Intrinsic glue distribution at very small x. *Phys. Rev. D* **55**, 5414–5428 (1997) <https://doi.org/10.1103/PhysRevD.55.5414> arXiv:hep-ph/9606337
- [33] Jalilian-Marian, J., Kovner, A., Leonidov, A., Weigert, H.: The BFKL equation from the Wilson renormalization group. *Nucl. Phys. B* **504**, 415–431 (1997) [https://doi.org/10.1016/S0550-3213\(97\)00440-9](https://doi.org/10.1016/S0550-3213(97)00440-9) arXiv:hep-ph/9701284
- [34] Jalilian-Marian, J., Kovner, A., Leonidov, A., Weigert, H.: The Wilson renormalization group for low x physics: Towards the high density regime. *Phys. Rev.*

- D **59**, 014014 (1998) <https://doi.org/10.1103/PhysRevD.59.014014> arXiv:hep-ph/9706377
- [35] Schenke, B., Tribedy, P., Venugopalan, R.: Fluctuating Glasma initial conditions and flow in heavy ion collisions. *Phys. Rev. Lett.* **108**, 252301 (2012) <https://doi.org/10.1103/PhysRevLett.108.252301> arXiv:1202.6646 [nucl-th]
- [36] Schenke, B., Tribedy, P., Venugopalan, R.: Event-by-event gluon multiplicity, energy density, and eccentricities in ultrarelativistic heavy-ion collisions. *Phys. Rev. C* **86**, 034908 (2012) <https://doi.org/10.1103/PhysRevC.86.034908> arXiv:1206.6805 [hep-ph]
- [37] Schenke, B., Schlichting, S.: 3D glasma initial state for relativistic heavy ion collisions. *Phys. Rev. C* **94**(4), 044907 (2016) <https://doi.org/10.1103/PhysRevC.94.044907> arXiv:1605.07158 [hep-ph]
- [38] Schenke, B., Shen, C., Tribedy, P.: Features of the IP-Glasma. *Nucl. Phys. A* **982**, 435–438 (2019) <https://doi.org/10.1016/j.nuclphysa.2018.08.015> arXiv:1807.05205 [nucl-th]
- [39] Dominguez, F., Marquet, C., Xiao, B.-W., Yuan, F.: Universality of Unintegrated Gluon Distributions at small x . *Phys. Rev. D* **83**, 105005 (2011) <https://doi.org/10.1103/PhysRevD.83.105005> arXiv:1101.0715 [hep-ph]
- [40] Mäntysaari, H., Schenke, B.: Evidence of strong proton shape fluctuations from incoherent diffraction. *Phys. Rev. Lett.* **117**(5), 052301 (2016) <https://doi.org/10.1103/PhysRevLett.117.052301> arXiv:1603.04349 [hep-ph]
- [41] Kowalski, H., Motyka, L., Watt, G.: Exclusive diffractive processes at HERA within the dipole picture. *Phys. Rev. D* **74**, 074016 (2006) <https://doi.org/10.1103/PhysRevD.74.074016> arXiv:hep-ph/0606272
- [42] Rezaeian, A.H., Siddikov, M., Klundert, M., Venugopalan, R.: Analysis of combined HERA data in the Impact-Parameter dependent Saturation model. *Phys. Rev. D* **87**(3), 034002 (2013) <https://doi.org/10.1103/PhysRevD.87.034002> arXiv:1212.2974 [hep-ph]
- [43] Demirci, S., Lappi, T., Schlichting, S.: Hot spots and gluon field fluctuations as causes of eccentricity in small systems. *Phys. Rev. D* **103**(9), 094025 (2021) <https://doi.org/10.1103/PhysRevD.103.094025> arXiv:2101.03791 [hep-ph]
- [44] Demirci, S., Lappi, T., Schlichting, S.: Proton hot spots and exclusive vector meson production. *Phys. Rev. D* **106**(7), 074025 (2022) <https://doi.org/10.1103/PhysRevD.106.074025> arXiv:2206.05207 [hep-ph]
- [45] Mäntysaari, H., Schenke, B.: Confronting impact parameter dependent JIMWLK evolution with HERA data. *Phys. Rev. D* **98**(3), 034013 (2018)

- <https://doi.org/10.1103/PhysRevD.98.034013> arXiv:1806.06783 [hep-ph]
- [46] Lappi, T., Schlichting, S.: Linearly polarized gluons and axial charge fluctuations in the Glasma. *Phys. Rev. D* **97**(3), 034034 (2018) <https://doi.org/10.1103/PhysRevD.97.034034> arXiv:1708.08625 [hep-ph]
- [47] Deganutti, F., Royon, C., Schlichting, S.: Forward dijet production at the LHC within an impact parameter dependent TMD approach. *JHEP* **01**, 159 (2024) [https://doi.org/10.1007/JHEP01\(2024\)159](https://doi.org/10.1007/JHEP01(2024)159) arXiv:2311.01965 [hep-ph]
- [48] Triantafyllopoulos, D.N.: The Energy dependence of the saturation momentum from RG improved BFKL evolution. *Nucl. Phys. B* **648**, 293–316 (2003) [https://doi.org/10.1016/S0550-3213\(02\)01000-3](https://doi.org/10.1016/S0550-3213(02)01000-3) arXiv:hep-ph/0209121
- [49] Kovner, A., Wiedemann, U.A.: Gluon radiation and parton energy loss, 192–248 (2003) https://doi.org/10.1142/9789812795533_0004 arXiv:hep-ph/0304151
- [50] Mäntysaari, H., Schenke, B., Shen, C., Zhao, W.: Bayesian inference of the fluctuating proton shape. *Phys. Lett. B* **833**, 137348 (2022) <https://doi.org/10.1016/j.physletb.2022.137348> arXiv:2202.01998 [hep-ph]
- [51] Schenke, B., Schlichting, S., Venugopalan, R.: Azimuthal anisotropies in p+Pb collisions from classical Yang–Mills dynamics. *Phys. Lett. B* **747**, 76–82 (2015) <https://doi.org/10.1016/j.physletb.2015.05.051> arXiv:1502.01331 [hep-ph]
- [52] Gribov, L.V., Levin, E.M., Ryskin, M.G.: Semihard Processes in QCD. *Phys. Rept.* **100**, 1–150 (1983) [https://doi.org/10.1016/0370-1573\(83\)90022-4](https://doi.org/10.1016/0370-1573(83)90022-4)
- [53] Kovchegov, Y.V., Levin, E.: *Quantum Chromodynamics at High Energy* vol. 33. Oxford University Press, ??? (2013). <https://doi.org/10.1017/9781009291446>
- [54] Aaron, F.D., *et al.*: Combined Measurement and QCD Analysis of the Inclusive e^+p Scattering Cross Sections at HERA. *JHEP* **01**, 109 (2010) [https://doi.org/10.1007/JHEP01\(2010\)109](https://doi.org/10.1007/JHEP01(2010)109) arXiv:0911.0884 [hep-ex]
- [55] Golec-Biernat, K.J., Wusthoff, M.: Saturation in diffractive deep inelastic scattering. *Phys. Rev. D* **60**, 114023 (1999) <https://doi.org/10.1103/PhysRevD.60.114023> arXiv:hep-ph/9903358
- [56] Kowalski, H., Teaney, D.: An Impact parameter dipole saturation model. *Phys. Rev. D* **68**, 114005 (2003) <https://doi.org/10.1103/PhysRevD.68.114005> arXiv:hep-ph/0304189
- [57] Salazar, F., Schenke, B.: Diffractive dijet production in impact parameter dependent saturation models. *Phys. Rev. D* **100**(3), 034007 (2019) <https://doi.org/10.1103/PhysRevD.100.034007> arXiv:1905.03763 [hep-ph]
- [58] Adloff, C., *et al.*: Elastic electroproduction of rho mesons at HERA. *Eur. Phys.*

- J. C **13**, 371–396 (2000) <https://doi.org/10.1007/s100520050703> arXiv:hep-ex/9902019
- [59] Chekanov, S., *et al.*: Exclusive electroproduction of phi mesons at HERA. Nucl. Phys. B **718**, 3–31 (2005) <https://doi.org/10.1016/j.nuclphysb.2005.04.009> arXiv:hep-ex/0504010
- [60] Chekanov, S., *et al.*: Exclusive electroproduction of J/psi mesons at HERA. Nucl. Phys. B **695**, 3–37 (2004) <https://doi.org/10.1016/j.nuclphysb.2004.06.034> arXiv:hep-ex/0404008
- [61] Aktas, A., *et al.*: Elastic J/psi production at HERA. Eur. Phys. J. C **46**, 585–603 (2006) <https://doi.org/10.1140/epjc/s2006-02519-5> arXiv:hep-ex/0510016
- [62] Good, M.L., Walker, W.D.: Diffraction dissociation of beam particles. Phys. Rev. **120**, 1857–1860 (1960) <https://doi.org/10.1103/PhysRev.120.1857>
- [63] Mäntysaari, H., Schenke, B.: Probing subnucleon scale fluctuations in ultraperipheral heavy ion collisions. Phys. Lett. B **772**, 832–838 (2017) <https://doi.org/10.1016/j.physletb.2017.07.063> arXiv:1703.09256 [hep-ph]
- [64] Gao, H., Vanderhaeghen, M.: The proton charge radius. Rev. Mod. Phys. **94**(1), 015002 (2022) <https://doi.org/10.1103/RevModPhys.94.015002> arXiv:2105.00571 [hep-ph]
- [65] Mäntysaari, H., Schenke, B.: Revealing proton shape fluctuations with incoherent diffraction at high energy. Phys. Rev. D **94**(3), 034042 (2016) <https://doi.org/10.1103/PhysRevD.94.034042> arXiv:1607.01711 [hep-ph]
- [66] Schlichting, S., Schenke, B.: The shape of the proton at high energies. Phys. Lett. B **739**, 313–319 (2014) <https://doi.org/10.1016/j.physletb.2014.10.068> arXiv:1407.8458 [hep-ph]
- [67] Mäntysaari, H., Schenke, B., Shen, C., Zhao, W.: Multiscale Imaging of Nuclear Deformation at the Electron-Ion Collider. Phys. Rev. Lett. **131**(6), 062301 (2023) <https://doi.org/10.1103/PhysRevLett.131.062301> arXiv:2303.04866 [nucl-th]
- [68] Mäntysaari, H., Salazar, F., Schenke, B., Shen, C., Zhao, W.: Effects of nuclear structure and quantum interference on diffractive vector meson production in ultraperipheral nuclear collisions. Phys. Rev. C **109**(2), 024908 (2024) <https://doi.org/10.1103/PhysRevC.109.024908> arXiv:2310.15300 [nucl-th]
- [69] Mäntysaari, H., Salazar, F., Schenke, B., Shen, C., Zhao, W.: Probing nuclear structure at the Electron-Ion Collider and in ultra-peripheral nuclear collisions. EPJ Web Conf. **296**, 10001 (2024) <https://doi.org/10.1051/epjconf/202429610001> arXiv:2312.07467 [nucl-th]

- [70] Baltz, A.J.: The Physics of Ultraperipheral Collisions at the LHC. Phys. Rept. **458**, 1–171 (2008) <https://doi.org/10.1016/j.physrep.2007.12.001> [arXiv:0706.3356](https://arxiv.org/abs/0706.3356) [nucl-ex]
- [71] Klein, S.R.: Ultra-peripheral collisions and hadronic structure. Nucl. Phys. A **967**, 249–256 (2017) <https://doi.org/10.1016/j.nuclphysa.2017.05.098> [arXiv:1704.04715](https://arxiv.org/abs/1704.04715) [nucl-ex]
- [72] Acharya, S., *et al.*: Neutron emission in ultraperipheral Pb-Pb collisions at $\sqrt{s_{NN}} = 5.02$ TeV. Phys. Rev. C **107**(6), 064902 (2023) <https://doi.org/10.1103/PhysRevC.107.064902> [arXiv:2209.04250](https://arxiv.org/abs/2209.04250) [nucl-ex]
- [73] Klein, S., Steinberg, P.: Photonuclear and Two-photon Interactions at High-Energy Nuclear Colliders. Ann. Rev. Nucl. Part. Sci. **70**, 323–354 (2020) <https://doi.org/10.1146/annurev-nucl-030320-033923> [arXiv:2005.01872](https://arxiv.org/abs/2005.01872) [nucl-ex]
- [74] Guzey, V., Strikman, M., Zhalov, M.: Disentangling coherent and incoherent quasielastic J/ψ photoproduction on nuclei by neutron tagging in ultraperipheral ion collisions at the LHC. Eur. Phys. J. C **74**(7), 2942 (2014) <https://doi.org/10.1140/epjc/s10052-014-2942-z> [arXiv:1312.6486](https://arxiv.org/abs/1312.6486) [hep-ph]
- [75] Abbas, E., *et al.*: Charmonium and e^+e^- pair photoproduction at mid-rapidity in ultra-peripheral Pb-Pb collisions at $\sqrt{s_{NN}}=2.76$ TeV. Eur. Phys. J. C **73**(11), 2617 (2013) <https://doi.org/10.1140/epjc/s10052-013-2617-1> [arXiv:1305.1467](https://arxiv.org/abs/1305.1467) [nucl-ex]
- [76] Acharya, S., *et al.*: First measurement of the $-t$ —dependence of coherent J/ψ photonuclear production. Phys. Lett. B **817**, 136280 (2021) <https://doi.org/10.1016/j.physletb.2021.136280> [arXiv:2101.04623](https://arxiv.org/abs/2101.04623) [nucl-ex]
- [77] Acharya, S., *et al.*: Energy dependence of coherent photonuclear production of J/ψ mesons in ultra-peripheral Pb-Pb collisions at $\sqrt{s_{NN}} = 5.02$ TeV. JHEP **10**, 119 (2023) [https://doi.org/10.1007/JHEP10\(2023\)119](https://doi.org/10.1007/JHEP10(2023)119) [arXiv:2305.19060](https://arxiv.org/abs/2305.19060) [nucl-ex]
- [78] Sirunyan, A.M., *et al.*: Measurement of exclusive $\rho(770)^0$ photoproduction in ultraperipheral pPb collisions at $\sqrt{s_{NN}} = 5.02$ TeV. Eur. Phys. J. C **79**(8), 702 (2019) <https://doi.org/10.1140/epjc/s10052-019-7202-9> [arXiv:1902.01339](https://arxiv.org/abs/1902.01339) [hep-ex]
- [79] Tumasyan, A., *et al.*: Probing Small Bjorken-x Nuclear Gluonic Structure via Coherent J/ψ Photoproduction in Ultraperipheral Pb-Pb Collisions at $s_{NN}=5.02$ TeV. Phys. Rev. Lett. **131**(26), 262301 (2023) <https://doi.org/10.1103/PhysRevLett.131.262301> [arXiv:2303.16984](https://arxiv.org/abs/2303.16984) [nucl-ex]
- [80] Aaij, R., *et al.*: Study of exclusive photoproduction of charmonium in ultra-peripheral lead-lead collisions. JHEP **06**, 146 (2023) <https://doi.org/10.1007/>

- [81] Abdulhamid, M.I., *et al.*: Observation of Strong Nuclear Suppression in Exclusive J/ψ Photoproduction in Au+Au Ultraperipheral Collisions at RHIC. *Phys. Rev. Lett.* **133**(5), 052301 (2024) <https://doi.org/10.1103/PhysRevLett.133.052301> arXiv:2311.13637 [nucl-ex]
- [82] Accardi, A., *et al.*: Electron Ion Collider: The Next QCD Frontier: Understanding the glue that binds us all. *Eur. Phys. J. A* **52**(9), 268 (2016) <https://doi.org/10.1140/epja/i2016-16268-9> arXiv:1212.1701 [nucl-ex]
- [83] Beuf, G., Hänninen, H., Lappi, T., Mäntysaari, H.: Color Glass Condensate at next-to-leading order meets HERA data. *Phys. Rev. D* **102**, 074028 (2020) <https://doi.org/10.1103/PhysRevD.102.074028> arXiv:2007.01645 [hep-ph]
- [84] Beuf, G., Lappi, T., Paatelainen, R.: Massive quarks in NLO dipole factorization for DIS: Longitudinal photon. *Phys. Rev. D* **104**(5), 056032 (2021) <https://doi.org/10.1103/PhysRevD.104.056032> arXiv:2103.14549 [hep-ph]
- [85] Balitsky, I., Chirilli, G.A.: Photon impact factor and k_T -factorization for DIS in the next-to-leading order. *Phys. Rev. D* **87**(1), 014013 (2013) <https://doi.org/10.1103/PhysRevD.87.014013> arXiv:1207.3844 [hep-ph]
- [86] Beuf, G.: NLO corrections for the dipole factorization of DIS structure functions at low x . *Phys. Rev. D* **85**, 034039 (2012) <https://doi.org/10.1103/PhysRevD.85.034039> arXiv:1112.4501 [hep-ph]
- [87] Beuf, G.: Dipole factorization for DIS at NLO: Loop correction to the $\gamma_{T,L}^* \rightarrow q\bar{q}$ light-front wave functions. *Phys. Rev. D* **94**(5), 054016 (2016) <https://doi.org/10.1103/PhysRevD.94.054016> arXiv:1606.00777 [hep-ph]
- [88] Beuf, G.: Dipole factorization for DIS at NLO: Combining the $q\bar{q}$ and $q\bar{q}g$ contributions. *Phys. Rev. D* **96**(7), 074033 (2017) <https://doi.org/10.1103/PhysRevD.96.074033> arXiv:1708.06557 [hep-ph]
- [89] Lappi, T., Paatelainen, R.: The one loop gluon emission light cone wave function. *Annals Phys.* **379**, 34–66 (2017) <https://doi.org/10.1016/j.aop.2017.02.002> arXiv:1611.00497 [hep-ph]
- [90] Hänninen, H., Lappi, T., Paatelainen, R.: One-loop corrections to light cone wave functions: the dipole picture DIS cross section. *Annals Phys.* **393**, 358–412 (2018) <https://doi.org/10.1016/j.aop.2018.04.015> arXiv:1711.08207 [hep-ph]
- [91] Ducloué, B., Hänninen, H., Lappi, T., Zhu, Y.: Deep inelastic scattering in the dipole picture at next-to-leading order. *Phys. Rev. D* **96**(9), 094017 (2017) <https://doi.org/10.1103/PhysRevD.96.094017> arXiv:1708.07328 [hep-ph]

- [92] Boussarie, R., Grabovsky, A.V., Ivanov, D.Y., Szymanowski, L., Wallon, S.: Next-to-Leading Order Computation of Exclusive Diffractive Light Vector Meson Production in a Saturation Framework. *Phys. Rev. Lett.* **119**(7), 072002 (2017) <https://doi.org/10.1103/PhysRevLett.119.072002> [arXiv:1612.08026](https://arxiv.org/abs/1612.08026) [hep-ph]
- [93] Boussarie, R., Grabovsky, A.V., Szymanowski, L., Wallon, S.: On the one loop $\gamma^{(*)} \rightarrow q\bar{q}$ impact factor and the exclusive diffractive cross sections for the production of two or three jets. *JHEP* **11**, 149 (2016) [https://doi.org/10.1007/JHEP11\(2016\)149](https://doi.org/10.1007/JHEP11(2016)149) [arXiv:1606.00419](https://arxiv.org/abs/1606.00419) [hep-ph]
- [94] Boussarie, R., Grabovsky, A.V., Szymanowski, L., Wallon, S.: Towards a complete next-to-logarithmic description of forward exclusive diffractive dijet electroproduction at HERA: real corrections. *Phys. Rev. D* **100**(7), 074020 (2019) <https://doi.org/10.1103/PhysRevD.100.074020> [arXiv:1905.07371](https://arxiv.org/abs/1905.07371) [hep-ph]
- [95] Caucal, P., Salazar, F., Schenke, B., Stebel, T., Venugopalan, R.: Back-to-back inclusive dijets in DIS at small x: gluon Weizsäcker-Williams distribution at NLO. *JHEP* **08**, 062 (2023) [https://doi.org/10.1007/JHEP08\(2023\)062](https://doi.org/10.1007/JHEP08(2023)062) [arXiv:2304.03304](https://arxiv.org/abs/2304.03304) [hep-ph]
- [96] Mäntysaari, H., Penttala, J.: Exclusive heavy vector meson production at next-to-leading order in the dipole picture. *Phys. Lett. B* **823**, 136723 (2021) <https://doi.org/10.1016/j.physletb.2021.136723> [arXiv:2104.02349](https://arxiv.org/abs/2104.02349) [hep-ph]
- [97] Mäntysaari, H., Penttala, J.: Exclusive production of light vector mesons at next-to-leading order in the dipole picture. *Phys. Rev. D* **105**(11), 114038 (2022) <https://doi.org/10.1103/PhysRevD.105.114038> [arXiv:2203.16911](https://arxiv.org/abs/2203.16911) [hep-ph]
- [98] Caucal, P., Salazar, F., Venugopalan, R.: Dijet impact factor in DIS at next-to-leading order in the Color Glass Condensate. *JHEP* **11**, 222 (2021) [https://doi.org/10.1007/JHEP11\(2021\)222](https://doi.org/10.1007/JHEP11(2021)222) [arXiv:2108.06347](https://arxiv.org/abs/2108.06347) [hep-ph]
- [99] Caucal, P., Salazar, F., Schenke, B., Stebel, T., Venugopalan, R.: Back-to-Back Inclusive Dijets in Deep Inelastic Scattering at Small x: Complete NLO Results and Predictions. *Phys. Rev. Lett.* **132**(8), 081902 (2024) <https://doi.org/10.1103/PhysRevLett.132.081902> [arXiv:2308.00022](https://arxiv.org/abs/2308.00022) [hep-ph]
- [100] Taels, P., Altinoluk, T., Beuf, G., Marquet, C.: Dijet photoproduction at low x at next-to-leading order and its back-to-back limit. *JHEP* **10**, 184 (2022) [https://doi.org/10.1007/JHEP10\(2022\)184](https://doi.org/10.1007/JHEP10(2022)184) [arXiv:2204.11650](https://arxiv.org/abs/2204.11650) [hep-ph]
- [101] Bergabo, F., Jalilian-Marian, J.: One-loop corrections to dihadron production in DIS at small x. *Phys. Rev. D* **106**(5), 054035 (2022) <https://doi.org/10.1103/PhysRevD.106.054035> [arXiv:2207.03606](https://arxiv.org/abs/2207.03606) [hep-ph]
- [102] Iancu, E., Mulian, Y.: Dihadron production in DIS at NLO: the real

- corrections. JHEP **07**, 121 (2023) [https://doi.org/10.1007/JHEP07\(2023\)121](https://doi.org/10.1007/JHEP07(2023)121) [arXiv:2211.04837](https://arxiv.org/abs/2211.04837) [hep-ph]
- [103] Caucal, P., Iancu, E.: The evolution of the transverse-momentum dependent gluon distribution at small x (2024) [arXiv:2406.04238](https://arxiv.org/abs/2406.04238) [hep-ph]
- [104] Bergabo, F., Jalilian-Marian, J.: Single inclusive hadron production in DIS at small x : next to leading order corrections. JHEP **01**, 095 (2023) [https://doi.org/10.1007/JHEP01\(2023\)095](https://doi.org/10.1007/JHEP01(2023)095) [arXiv:2210.03208](https://arxiv.org/abs/2210.03208) [hep-ph]
- [105] Altinoluk, T., Jalilian-Marian, J., Marquet, C.: Sudakov double logs in single-inclusive hadron production in DIS at small x from the color glass condensate formalism. Phys. Rev. D **110**(9), 094056 (2024) <https://doi.org/10.1103/PhysRevD.110.094056> [arXiv:2406.08277](https://arxiv.org/abs/2406.08277) [hep-ph]
- [106] Caucal, P., Iancu, E., Mueller, A.H., Yuan, F.: Jet definition and TMD factorisation in SIDIS (2024) [arXiv:2408.03129](https://arxiv.org/abs/2408.03129) [hep-ph]
- [107] Beuf, G., Lappi, T., Mäntysaari, H., Paatelainen, R., Penttala, J.: Diffractive deep inelastic scattering at NLO in the dipole picture. JHEP **05**, 024 (2024) [https://doi.org/10.1007/JHEP05\(2024\)024](https://doi.org/10.1007/JHEP05(2024)024) [arXiv:2401.17251](https://arxiv.org/abs/2401.17251) [hep-ph]
- [108] Iancu, E., Mueller, A.H., Triantafyllopoulos, D.N.: Probing Parton Saturation and the Gluon Dipole via Diffractive Jet Production at the Electron-Ion Collider. Phys. Rev. Lett. **128**(20), 202001 (2022) <https://doi.org/10.1103/PhysRevLett.128.202001> [arXiv:2112.06353](https://arxiv.org/abs/2112.06353) [hep-ph]
- [109] Hatta, Y., Xiao, B.-W., Yuan, F.: Semi-inclusive diffractive deep inelastic scattering at small x . Phys. Rev. D **106**(9), 094015 (2022) <https://doi.org/10.1103/PhysRevD.106.094015> [arXiv:2205.08060](https://arxiv.org/abs/2205.08060) [hep-ph]
- [110] Iancu, E., Mueller, A.H., Triantafyllopoulos, D.N., Wei, S.Y.: Probing gluon saturation via diffractive jets in ultra-peripheral nucleus-nucleus collisions. Eur. Phys. J. C **83**(11), 1078 (2023) <https://doi.org/10.1140/epjc/s10052-023-12165-8> [arXiv:2304.12401](https://arxiv.org/abs/2304.12401) [hep-ph]
- [111] Morreale, A., Salazar, F.: Mining for Gluon Saturation at Colliders. Universe **7**(8), 312 (2021) <https://doi.org/10.3390/universe7080312> [arXiv:2108.08254](https://arxiv.org/abs/2108.08254) [hep-ph]
- [112] Dumitru, A., Hayashigaki, A., Jalilian-Marian, J.: The Color glass condensate and hadron production in the forward region. Nucl. Phys. A **765**, 464–482 (2006) <https://doi.org/10.1016/j.nuclphysa.2005.11.014> [arXiv:hep-ph/0506308](https://arxiv.org/abs/hep-ph/0506308)
- [113] Albacete, J.L., Dumitru, A., Marquet, C.: The initial state of heavy-ion collisions. Int. J. Mod. Phys. A **28**, 1340010 (2013) <https://doi.org/10.1142/S0217751X13400101> [arXiv:1302.6433](https://arxiv.org/abs/1302.6433) [hep-ph]

- [114] Albacete, J.L., Marquet, C.: Gluon saturation and initial conditions for relativistic heavy ion collisions. *Prog. Part. Nucl. Phys.* **76**, 1–42 (2014) <https://doi.org/10.1016/j.ppnp.2014.01.004> arXiv:1401.4866 [hep-ph]
- [115] Dumitru, A., Jalilian-Marian, J.: Scattering of gluons from the color glass condensate. *Phys. Lett. B* **547**, 15–20 (2002) [https://doi.org/10.1016/S0370-2693\(02\)02709-0](https://doi.org/10.1016/S0370-2693(02)02709-0) arXiv:hep-ph/0111357
- [116] Lappi, T., Mantysaari, H.: Forward dihadron correlations in deuteron-gold collisions with the Gaussian approximation of JIMWLK. *Nucl. Phys. A* **908**, 51–72 (2013) <https://doi.org/10.1016/j.nuclphysa.2013.03.017> arXiv:1209.2853 [hep-ph]
- [117] Chirilli, G.A., Xiao, B.-W., Yuan, F.: Inclusive Hadron Productions in pA Collisions. *Phys. Rev. D* **86**, 054005 (2012) <https://doi.org/10.1103/PhysRevD.86.054005> arXiv:1203.6139 [hep-ph]
- [118] Chirilli, G.A., Xiao, B.-W., Yuan, F.: One-loop Factorization for Inclusive Hadron Production in pA Collisions in the Saturation Formalism. *Phys. Rev. Lett.* **108**, 122301 (2012) <https://doi.org/10.1103/PhysRevLett.108.122301> arXiv:1112.1061 [hep-ph]
- [119] Lappi, T., Mäntysaari, H.: Single inclusive particle production at high energy from HERA data to proton-nucleus collisions. *Phys. Rev. D* **88**, 114020 (2013) <https://doi.org/10.1103/PhysRevD.88.114020> arXiv:1309.6963 [hep-ph]
- [120] Iancu, E., Mulian, Y.: Forward dijets in proton-nucleus collisions at next-to-leading order: the real corrections. *JHEP* **03**, 005 (2021) [https://doi.org/10.1007/JHEP03\(2021\)005](https://doi.org/10.1007/JHEP03(2021)005) arXiv:2009.11930 [hep-ph]
- [121] Gelis, F., Jalilian-Marian, J.: Dilepton production from the color glass condensate. *Phys. Rev. D* **66**, 094014 (2002) <https://doi.org/10.1103/PhysRevD.66.094014> arXiv:hep-ph/0208141
- [122] Gelis, F., Jalilian-Marian, J.: Photon production in high-energy proton nucleus collisions. *Phys. Rev. D* **66**, 014021 (2002) <https://doi.org/10.1103/PhysRevD.66.014021> arXiv:hep-ph/0205037
- [123] Benić, S., Fukushima, K., Garcia-Montero, O., Venugopalan, R.: Constraining unintegrated gluon distributions from inclusive photon production in proton–proton collisions at the LHC. *Phys. Lett. B* **791**, 11–16 (2019) <https://doi.org/10.1016/j.physletb.2019.02.007> arXiv:1807.03806 [hep-ph]
- [124] Benic, S., Fukushima, K., Garcia-Montero, O., Venugopalan, R.: Probing gluon saturation with next-to-leading order photon production at central rapidities in proton-nucleus collisions. *JHEP* **01**, 115 (2017) [https://doi.org/10.1007/JHEP01\(2017\)115](https://doi.org/10.1007/JHEP01(2017)115) arXiv:1609.09424 [hep-ph]

- [125] Benić, S., Garcia-Montero, O., Perkov, A.: Isolated photon-hadron production in high energy pp and pA collisions at RHIC and LHC. *Phys. Rev. D* **105**(11), 114052 (2022) <https://doi.org/10.1103/PhysRevD.105.114052> arXiv:2203.01685 [hep-ph]
- [126] Placakyte, R.: Parton Distribution Functions. In: 31st International Symposium on Physics In Collision (2011)
- [127] Aidala, C., *et al.*: Nuclear-modification factor of charged hadrons at forward and backward rapidity in p +Al and p +Au collisions at $\sqrt{s_{NN}} = 200$ GeV. *Phys. Rev. C* **101**(3), 034910 (2020) <https://doi.org/10.1103/PhysRevC.101.034910> arXiv:1906.09928 [hep-ex]
- [128] Abelev, B., *et al.*: Transverse momentum distribution and nuclear modification factor of charged particles in p -Pb collisions at $\sqrt{s_{NN}} = 5.02$ TeV. *Phys. Rev. Lett.* **110**(8), 082302 (2013) <https://doi.org/10.1103/PhysRevLett.110.082302> arXiv:1210.4520 [nucl-ex]
- [129] Marquet, C.: Forward inclusive dijet production and azimuthal correlations in p(A) collisions. *Nucl. Phys. A* **796**, 41–60 (2007) <https://doi.org/10.1016/j.nuclphysa.2007.09.001> arXiv:0708.0231 [hep-ph]
- [130] Stasto, A., Xiao, B.-W., Yuan, F.: Back-to-Back Correlations of Di-hadrons in dAu Collisions at RHIC. *Phys. Lett. B* **716**, 430–434 (2012) <https://doi.org/10.1016/j.physletb.2012.08.044> arXiv:1109.1817 [hep-ph]
- [131] Albacete, J.L., Marquet, C.: Azimuthal correlations of forward di-hadrons in d+Au collisions at RHIC in the Color Glass Condensate. *Phys. Rev. Lett.* **105**, 162301 (2010) <https://doi.org/10.1103/PhysRevLett.105.162301> arXiv:1005.4065 [hep-ph]
- [132] Iancu, E., Laidet, J.: Gluon splitting in a shockwave. *Nucl. Phys. A* **916**, 48–78 (2013) <https://doi.org/10.1016/j.nuclphysa.2013.07.012> arXiv:1305.5926 [hep-ph]
- [133] Hameren, A., Kotko, P., Kutak, K., Marquet, C., Petreska, E., Sapeta, S.: Forward di-jet production in p+Pb collisions in the small-x improved TMD factorization framework. *JHEP* **12**, 034 (2016) [https://doi.org/10.1007/JHEP12\(2016\)034](https://doi.org/10.1007/JHEP12(2016)034) arXiv:1607.03121 [hep-ph]. [Erratum: *JHEP* 02, 158 (2019)]
- [134] Fujii, H., Marquet, C., Watanabe, K.: Comparison of improved TMD and CGC frameworks in forward quark dijet production. *JHEP* **12**, 181 (2020) [https://doi.org/10.1007/JHEP12\(2020\)181](https://doi.org/10.1007/JHEP12(2020)181) arXiv:2006.16279 [hep-ph]
- [135] Hameren, A., Kakkad, H., Kotko, P., Kutak, K., Sapeta, S.: Searching for saturation in forward dijet production at the LHC. *Eur. Phys. J. C* **83**(10), 947 (2023) <https://doi.org/10.1140/epjc/s10052-023-12120-7> arXiv:2306.17513 [hep-ph]

- [136] Adare, A., *et al.*: Suppression of back-to-back hadron pairs at forward rapidity in $d+\text{Au}$ Collisions at $\sqrt{s_{NN}} = 200$ GeV. *Phys. Rev. Lett.* **107**, 172301 (2011) <https://doi.org/10.1103/PhysRevLett.107.172301> arXiv:1105.5112 [nucl-ex]
- [137] Braidot, E.: Suppression of Forward Pion Correlations in $d+\text{Au}$ Interactions at STAR. In: 45th Rencontres de Moriond on QCD and High Energy Interactions, pp. 355–338 (2010)
- [138] Aaboud, M., *et al.*: Dijet azimuthal correlations and conditional yields in pp and $p+\text{Pb}$ collisions at $s_{NN}=5.02\text{TeV}$ with the ATLAS detector. *Phys. Rev. C* **100**(3), 034903 (2019) <https://doi.org/10.1103/PhysRevC.100.034903> arXiv:1901.10440 [nucl-ex]
- [139] Aad, G., *et al.*: Measurement of the inclusive isolated prompt photon cross section in pp collisions at $\sqrt{s} = 7$ TeV with the ATLAS detector. *Phys. Rev. D* **83**, 052005 (2011) <https://doi.org/10.1103/PhysRevD.83.052005> arXiv:1012.4389 [hep-ex]
- [140] Chatrchyan, S., *et al.*: Measurement of Isolated Photon Production in pp and PbPb Collisions at $\sqrt{s_{NN}} = 2.76$ TeV. *Phys. Lett. B* **710**, 256–277 (2012) <https://doi.org/10.1016/j.physletb.2012.02.077> arXiv:1201.3093 [nucl-ex]
- [141] Khachatryan, V., *et al.*: Measurement of the Isolated Prompt Photon Production Cross Section in pp Collisions at $\sqrt{s} = 7$ TeV. *Phys. Rev. Lett.* **106**, 082001 (2011) <https://doi.org/10.1103/PhysRevLett.106.082001> arXiv:1012.0799 [hep-ex]
- [142] Chatrchyan, S., *et al.*: Measurement of the Differential Cross Section for Isolated Prompt Photon Production in pp Collisions at 7 TeV. *Phys. Rev. D* **84**, 052011 (2011) <https://doi.org/10.1103/PhysRevD.84.052011> arXiv:1108.2044 [hep-ex]
- [143] Benic, S., Fukushima, K.: Photon from the annihilation process with CGC in the pA collision. *Nucl. Phys. A* **958**, 1–24 (2017) <https://doi.org/10.1016/j.nuclphysa.2016.11.003> arXiv:1602.01989 [hep-ph]
- [144] Jalilian-Marian, J., Rezaeian, A.H.: Prompt photon production and photon-hadron correlations at RHIC and the LHC from the Color Glass Condensate. *Phys. Rev. D* **86**, 034016 (2012) <https://doi.org/10.1103/PhysRevD.86.034016> arXiv:1204.1319 [hep-ph]
- [145] Roy, K., Venugopalan, R.: NLO impact factor for inclusive photon+dijet production in $e + A$ DIS at small x . *Phys. Rev. D* **101**(3), 034028 (2020) <https://doi.org/10.1103/PhysRevD.101.034028> arXiv:1911.04530 [hep-ph]
- [146] Roy, K., Venugopalan, R.: Extracting many-body correlators of saturated gluons with precision from inclusive photon+dijet final states in deeply inelastic scattering. *Phys. Rev. D* **101**(7), 071505 (2020) <https://doi.org/10.1103/PhysRevD.101.071505>

101.071505 arXiv:1911.04519 [hep-ph]

- [147] Altinoluk, T., Boussarie, R., Marquet, C., Taels, P.: TMD factorization for dijets + photon production from the dilute-dense CGC framework. *JHEP* **07**, 079 (2019) [https://doi.org/10.1007/JHEP07\(2019\)079](https://doi.org/10.1007/JHEP07(2019)079) arXiv:1810.11273 [hep-ph]
- [148] Altinoluk, T., Armesto, N., Beuf, G., Kovner, A., Lublinsky, M.: Single-inclusive particle production in proton-nucleus collisions at next-to-leading order in the hybrid formalism. *Phys. Rev. D* **91**(9), 094016 (2015) <https://doi.org/10.1103/PhysRevD.91.094016> arXiv:1411.2869 [hep-ph]
- [149] Ducloué, B., Lappi, T., Zhu, Y.: Single inclusive forward hadron production at next-to-leading order. *Phys. Rev. D* **93**(11), 114016 (2016) <https://doi.org/10.1103/PhysRevD.93.114016> arXiv:1604.00225 [hep-ph]
- [150] Stasto, A.M., Xiao, B.-W., Zaslavsky, D.: Towards the Test of Saturation Physics Beyond Leading Logarithm. *Phys. Rev. Lett.* **112**(1), 012302 (2014) <https://doi.org/10.1103/PhysRevLett.112.012302> arXiv:1307.4057 [hep-ph]
- [151] Shi, Y., Wang, L., Wei, S.-Y., Xiao, B.-W.: Pursuing the Precision Study for Color Glass Condensate in Forward Hadron Productions. *Phys. Rev. Lett.* **128**(20), 202302 (2022) <https://doi.org/10.1103/PhysRevLett.128.202302> arXiv:2112.06975 [hep-ph]
- [152] Iancu, E., Mueller, A.H., Triantafyllopoulos, D.N.: CGC factorization for forward particle production in proton-nucleus collisions at next-to-leading order. *JHEP* **12**, 041 (2016) [https://doi.org/10.1007/JHEP12\(2016\)041](https://doi.org/10.1007/JHEP12(2016)041) arXiv:1608.05293 [hep-ph]
- [153] Ducloué, B., Lappi, T., Zhu, Y.: Implementation of NLO high energy factorization in single inclusive forward hadron production. *Phys. Rev. D* **95**(11), 114007 (2017) <https://doi.org/10.1103/PhysRevD.95.114007> arXiv:1703.04962 [hep-ph]
- [154] Balitsky, I., Chirilli, G.A.: Next-to-leading order evolution of color dipoles. *Phys. Rev. D* **77**, 014019 (2008) <https://doi.org/10.1103/PhysRevD.77.014019> arXiv:0710.4330 [hep-ph]
- [155] Iancu, E., Lappi, T., Triantafyllopoulos, D.: Small- x Physics in the Dipole Picture at NLO Accuracy. In: *Probing Nucleons and Nuclei in High Energy Collisions: Dedicated to the Physics of the Electron Ion Collider*, pp. 274–294 (2020). https://doi.org/10.1142/9789811214950_0055
- [156] Kovner, A., Lublinsky, M., Mulian, Y.: Jalilian-Marian, Iancu, McLerran, Weigert, Leonidov, Kovner evolution at next to leading order. *Phys. Rev. D* **89**(6), 061704 (2014) <https://doi.org/10.1103/PhysRevD.89.061704> arXiv:1310.0378 [hep-ph]

- [157] Balitsky, I., Chirilli, G.A.: Rapidity evolution of Wilson lines at the next-to-leading order. *Phys. Rev. D* **88**, 111501 (2013) <https://doi.org/10.1103/PhysRevD.88.111501> [arXiv:1309.7644](https://arxiv.org/abs/1309.7644) [hep-ph]
- [158] Lublinsky, M., Mulian, Y.: High Energy QCD at NLO: from light-cone wave function to JIMWLK evolution. *JHEP* **05**, 097 (2017) [https://doi.org/10.1007/JHEP05\(2017\)097](https://doi.org/10.1007/JHEP05(2017)097) [arXiv:1610.03453](https://arxiv.org/abs/1610.03453) [hep-ph]
- [159] Kovner, A., Lublinsky, M., Mulian, Y.: NLO JIMWLK evolution unabridged. *JHEP* **08**, 114 (2014) [https://doi.org/10.1007/JHEP08\(2014\)114](https://doi.org/10.1007/JHEP08(2014)114) [arXiv:1405.0418](https://arxiv.org/abs/1405.0418) [hep-ph]
- [160] Dai, L., Lublinsky, M.: NLO JIMWLK evolution with massive quarks. *JHEP* **07**, 093 (2022) [https://doi.org/10.1007/JHEP07\(2022\)093](https://doi.org/10.1007/JHEP07(2022)093) [arXiv:2203.13695](https://arxiv.org/abs/2203.13695) [hep-ph]
- [161] Beuf, G.: Improving the kinematics for low- x QCD evolution equations in coordinate space. *Phys. Rev. D* **89**(7), 074039 (2014) <https://doi.org/10.1103/PhysRevD.89.074039> [arXiv:1401.0313](https://arxiv.org/abs/1401.0313) [hep-ph]
- [162] Iancu, E., Madrigal, J.D., Mueller, A.H., Soyez, G., Triantafyllopoulos, D.N.: Resumming double logarithms in the QCD evolution of color dipoles. *Phys. Lett. B* **744**, 293–302 (2015) <https://doi.org/10.1016/j.physletb.2015.03.068> [arXiv:1502.05642](https://arxiv.org/abs/1502.05642) [hep-ph]
- [163] Ducloué, B., Iancu, E., Mueller, A.H., Soyez, G., Triantafyllopoulos, D.N.: Non-linear evolution in QCD at high-energy beyond leading order. *JHEP* **04**, 081 (2019) [https://doi.org/10.1007/JHEP04\(2019\)081](https://doi.org/10.1007/JHEP04(2019)081) [arXiv:1902.06637](https://arxiv.org/abs/1902.06637) [hep-ph]
- [164] Lappi, T., Mäntysaari, H.: Next-to-leading order Balitsky-Kovchegov equation with resummation. *Phys. Rev. D* **93**(9), 094004 (2016) <https://doi.org/10.1103/PhysRevD.93.094004> [arXiv:1601.06598](https://arxiv.org/abs/1601.06598) [hep-ph]
- [165] Elfner, H., Müller, B.: The exploration of hot and dense nuclear matter: introduction to relativistic heavy-ion physics. *J. Phys. G* **50**(10), 103001 (2023) <https://doi.org/10.1088/1361-6471/ace824> [arXiv:2210.12056](https://arxiv.org/abs/2210.12056) [nucl-th]
- [166] Berges, J., Heller, M.P., Mazeliauskas, A., Venugopalan, R.: QCD thermalization: Ab initio approaches and interdisciplinary connections. *Rev. Mod. Phys.* **93**(3), 035003 (2021) <https://doi.org/10.1103/RevModPhys.93.035003> [arXiv:2005.12299](https://arxiv.org/abs/2005.12299) [hep-th]
- [167] Gelis, F., Lappi, T., Venugopalan, R.: High energy scattering in Quantum Chromodynamics. *Int. J. Mod. Phys. E* **16**, 2595–2637 (2007) <https://doi.org/10.1142/S0218301307008331> [arXiv:0708.0047](https://arxiv.org/abs/0708.0047) [hep-ph]
- [168] Ipp, A., Müller, D.I., Schlichting, S., Singh, P.: Spacetime structure of (3+1)D

- color fields in high energy nuclear collisions. *Phys. Rev. D* **104**(11), 114040 (2021) <https://doi.org/10.1103/PhysRevD.104.114040> [arXiv:2109.05028](https://arxiv.org/abs/2109.05028) [hep-ph]
- [169] Ipp, A., Leuthner, M., Müller, D.I., Schlichting, S., Schmidt, K., Singh, P.: Energy-momentum tensor of the dilute (3+1)D glasma. *Phys. Rev. D* **109**(9), 094040 (2024) <https://doi.org/10.1103/PhysRevD.109.094040> [arXiv:2401.10320](https://arxiv.org/abs/2401.10320) [hep-ph]
- [170] Ipp, A., Müller, D.I.: Progress on 3+1D Glasma simulations. *Eur. Phys. J. A* **56**(9), 243 (2020) <https://doi.org/10.1140/epja/s10050-020-00241-6> [arXiv:2009.02044](https://arxiv.org/abs/2009.02044) [hep-ph]
- [171] Ipp, A., Müller, D.I., Schuh, D.: On transverse momentum broadening in real-time lattice simulations of the glasma and in the weak-field limit. *EPJ Web Conf.* **258**, 05002 (2022) <https://doi.org/10.1051/epjconf/202225805002> [arXiv:2112.03883](https://arxiv.org/abs/2112.03883) [hep-ph]
- [172] Schlichting, S., Singh, P.: 3-D structure of the Glasma initial state – Breaking boost-invariance by collisions of extended shock waves in classical Yang-Mills theory. *Phys. Rev. D* **103**(1), 014003 (2021) <https://doi.org/10.1103/PhysRevD.103.014003> [arXiv:2010.11172](https://arxiv.org/abs/2010.11172) [hep-ph]
- [173] Dusling, K., Gelis, F., Venugopalan, R.: The initial spectrum of fluctuations in the little bang. *Nucl. Phys. A* **872**, 161–195 (2011) <https://doi.org/10.1016/j.nuclphysa.2011.09.012> [arXiv:1106.3927](https://arxiv.org/abs/1106.3927) [nucl-th]
- [174] Epelbaum, T., Gelis, F.: Fluctuations of the initial color fields in high energy heavy ion collisions. *Phys. Rev. D* **88**, 085015 (2013) <https://doi.org/10.1103/PhysRevD.88.085015> [arXiv:1307.1765](https://arxiv.org/abs/1307.1765) [hep-ph]
- [175] Gelis, F., Schenke, B.: Initial State Quantum Fluctuations in the Little Bang. *Ann. Rev. Nucl. Part. Sci.* **66**, 73–94 (2016) <https://doi.org/10.1146/annurev-nucl-102115-044651> [arXiv:1604.00335](https://arxiv.org/abs/1604.00335) [hep-ph]
- [176] Kovner, A., McLerran, L.D., Weigert, H.: Gluon production from nonAbelian Weizsacker-Williams fields in nucleus-nucleus collisions. *Phys. Rev. D* **52**, 6231–6237 (1995) <https://doi.org/10.1103/PhysRevD.52.6231> [arXiv:hep-ph/9502289](https://arxiv.org/abs/hep-ph/9502289)
- [177] Kovner, A., McLerran, L.D., Weigert, H.: Gluon production at high transverse momentum in the McLerran-Venugopalan model of nuclear structure functions. *Phys. Rev. D* **52**, 3809–3814 (1995) <https://doi.org/10.1103/PhysRevD.52.3809> [arXiv:hep-ph/9505320](https://arxiv.org/abs/hep-ph/9505320)
- [178] Lappi, T., McLerran, L.: Some features of the glasma. *Nucl. Phys. A* **772**, 200–212 (2006) <https://doi.org/10.1016/j.nuclphysa.2006.04.001> [arXiv:hep-ph/0602189](https://arxiv.org/abs/hep-ph/0602189)

- [179] Carrington, M.E., Czajka, A., Mrówczyński, S.: Physical characteristics of glasma from the earliest stage of relativistic heavy ion collisions. *Phys. Rev. C* **106**(3), 034904 (2022) <https://doi.org/10.1103/PhysRevC.106.034904> [arXiv:2105.05327](https://arxiv.org/abs/2105.05327) [hep-ph]
- [180] Carrington, M.E., Czajka, A., Mrowczynski, S.: The energy-momentum tensor at the earliest stage of relativistic heavy-ion collisions. *Eur. Phys. J. A* **58**(1), 5 (2022) <https://doi.org/10.1140/epja/s10050-021-00600-x> [arXiv:2012.03042](https://arxiv.org/abs/2012.03042) [hep-ph]
- [181] Krasnitz, A., Venugopalan, R.: Nonperturbative computation of gluon minijet production in nuclear collisions at very high-energies. *Nucl. Phys. B* **557**, 237 (1999) [https://doi.org/10.1016/S0550-3213\(99\)00366-1](https://doi.org/10.1016/S0550-3213(99)00366-1) [arXiv:hep-ph/9809433](https://arxiv.org/abs/hep-ph/9809433)
- [182] Lappi, T.: Production of gluons in the classical field model for heavy ion collisions. *Phys. Rev. C* **67**, 054903 (2003) <https://doi.org/10.1103/PhysRevC.67.054903> [arXiv:hep-ph/0303076](https://arxiv.org/abs/hep-ph/0303076)
- [183] Lappi, T.: Gluon spectrum in the glasma from JIMWLK evolution. *Phys. Lett. B* **703**, 325–330 (2011) <https://doi.org/10.1016/j.physletb.2011.08.011> [arXiv:1105.5511](https://arxiv.org/abs/1105.5511) [hep-ph]
- [184] Dumitru, A., McLerran, L.D.: How protons shatter colored glass. *Nucl. Phys. A* **700**, 492–508 (2002) [https://doi.org/10.1016/S0375-9474\(01\)01301-X](https://doi.org/10.1016/S0375-9474(01)01301-X) [arXiv:hep-ph/0105268](https://arxiv.org/abs/hep-ph/0105268)
- [185] Gale, C., Jeon, S., Schenke, B., Tribedy, P., Venugopalan, R.: Event-by-event anisotropic flow in heavy-ion collisions from combined Yang-Mills and viscous fluid dynamics. *Phys. Rev. Lett.* **110**(1), 012302 (2013) <https://doi.org/10.1103/PhysRevLett.110.012302> [arXiv:1209.6330](https://arxiv.org/abs/1209.6330) [nucl-th]
- [186] Baier, R., Mueller, A.H., Schiff, D., Son, D.T.: 'Bottom up' thermalization in heavy ion collisions. *Phys. Lett. B* **502**, 51–58 (2001) [https://doi.org/10.1016/S0370-2693\(01\)00191-5](https://doi.org/10.1016/S0370-2693(01)00191-5) [arXiv:hep-ph/0009237](https://arxiv.org/abs/hep-ph/0009237)
- [187] Kurkela, A., Zhu, Y.: Isotropization and hydrodynamization in weakly coupled heavy-ion collisions. *Phys. Rev. Lett.* **115**(18), 182301 (2015) <https://doi.org/10.1103/PhysRevLett.115.182301> [arXiv:1506.06647](https://arxiv.org/abs/1506.06647) [hep-ph]
- [188] Keegan, L., Kurkela, A., Romatschke, P., Schee, W., Zhu, Y.: Weak and strong coupling equilibration in nonabelian gauge theories. *JHEP* **04**, 031 (2016) [https://doi.org/10.1007/JHEP04\(2016\)031](https://doi.org/10.1007/JHEP04(2016)031) [arXiv:1512.05347](https://arxiv.org/abs/1512.05347) [hep-th]
- [189] Schlichting, S., Teaney, D.: The First fm/c of Heavy-Ion Collisions. *Ann. Rev. Nucl. Part. Sci.* **69**, 447–476 (2019) <https://doi.org/10.1146/annurev-nucl-101918-023825> [arXiv:1908.02113](https://arxiv.org/abs/1908.02113) [nucl-th]

- [190] Giacalone, G., Mazeliauskas, A., Schlichting, S.: Hydrodynamic attractors, initial state energy and particle production in relativistic nuclear collisions. *Phys. Rev. Lett.* **123**(26), 262301 (2019) <https://doi.org/10.1103/PhysRevLett.123.262301> [arXiv:1908.02866](https://arxiv.org/abs/1908.02866) [hep-ph]
- [191] Giacalone, G., Schenke, B., Shen, C.: Observable signatures of initial state momentum anisotropies in nuclear collisions. *Phys. Rev. Lett.* **125**(19), 192301 (2020) <https://doi.org/10.1103/PhysRevLett.125.192301> [arXiv:2006.15721](https://arxiv.org/abs/2006.15721) [nucl-th]
- [192] Greif, M., Greiner, C., Schenke, B., Schlichting, S., Xu, Z.: Importance of initial and final state effects for azimuthal correlations in p+Pb collisions. *Phys. Rev. D* **96**(9), 091504 (2017) <https://doi.org/10.1103/PhysRevD.96.091504> [arXiv:1708.02076](https://arxiv.org/abs/1708.02076) [hep-ph]
- [193] Schenke, B., Shen, C., Tribedy, P.: Hybrid Color Glass Condensate and hydrodynamic description of the Relativistic Heavy Ion Collider small system scan. *Phys. Lett. B* **803**, 135322 (2020) <https://doi.org/10.1016/j.physletb.2020.135322> [arXiv:1908.06212](https://arxiv.org/abs/1908.06212) [nucl-th]
- [194] Schenke, B., Schlichting, S., Singh, P.: Rapidity dependence of initial state geometry and momentum correlations in p+Pb collisions. *Phys. Rev. D* **105**(9), 094023 (2022) <https://doi.org/10.1103/PhysRevD.105.094023> [arXiv:2201.08864](https://arxiv.org/abs/2201.08864) [nucl-th]
- [195] Mace, M., Skokov, V.V., Tribedy, P., Venugopalan, R.: Hierarchy of Azimuthal Anisotropy Harmonics in Collisions of Small Systems from the Color Glass Condensate. *Phys. Rev. Lett.* **121**(5), 052301 (2018) <https://doi.org/10.1103/PhysRevLett.121.052301> [arXiv:1805.09342](https://arxiv.org/abs/1805.09342) [hep-ph]. [Erratum: *Phys.Rev.Lett.* **123**, 039901 (2019)]
- [196] Niemi, H., Eskola, K.J., Paatelainen, R.: Event-by-event fluctuations in a perturbative QCD + saturation + hydrodynamics model: Determining QCD matter shear viscosity in ultrarelativistic heavy-ion collisions. *Phys. Rev. C* **93**(2), 024907 (2016) <https://doi.org/10.1103/PhysRevC.93.024907> [arXiv:1505.02677](https://arxiv.org/abs/1505.02677) [hep-ph]
- [197] Kuha, M., Auvinen, J., Eskola, K.J., Hirvonen, H., Kanakubo, Y., Niemi, H.: MC-EKRT: Monte Carlo event generator with saturated minijet production for initializing 3+1 D fluid dynamics in high energy nuclear collisions (2024) [arXiv:2406.17592](https://arxiv.org/abs/2406.17592) [hep-ph]
- [198] Moreland, J.S., Bernhard, J.E., Bass, S.A.: Alternative ansatz to wounded nucleon and binary collision scaling in high-energy nuclear collisions. *Phys. Rev. C* **92**(1), 011901 (2015) <https://doi.org/10.1103/PhysRevC.92.011901> [arXiv:1412.4708](https://arxiv.org/abs/1412.4708) [nucl-th]

- [199] Nijs, G., Schee, W., Gürsoy, U., Snellings, R.: Transverse Momentum Differential Global Analysis of Heavy-Ion Collisions. *Phys. Rev. Lett.* **126**(20), 202301 (2021) <https://doi.org/10.1103/PhysRevLett.126.202301> arXiv:2010.15130 [nucl-th]
- [200] Bożek, P., Broniowski, W.: Collective Dynamics in Small Systems. *Acta Phys. Polon. Supp.* **10**, 501–505 (2017) <https://doi.org/10.5506/APhysPolBSupp.10.501>
- [201] Ambrus, V.E., Schlichting, S., Werthmann, C.: Establishing the Range of Applicability of Hydrodynamics in High-Energy Collisions. *Phys. Rev. Lett.* **130**(15), 152301 (2023) <https://doi.org/10.1103/PhysRevLett.130.152301> arXiv:2211.14356 [hep-ph]
- [202] Cao, R.-X., Zhang, S., Ma, Y.-G.: Effects of the α -cluster structure and the intrinsic momentum component of nuclei on the longitudinal asymmetry in relativistic heavy-ion collisions. *Phys. Rev. C* **108**(6), 064906 (2023) <https://doi.org/10.1103/PhysRevC.108.064906> arXiv:2308.16636 [hep-ph]
- [203] Ding, C., Pang, L.-G., Zhang, S., Ma, Y.-G.: Signals of α clusters in $^{16}\text{O}+^{16}\text{O}$ collisions at the LHC from relativistic hydrodynamic simulations. *Chin. Phys. C* **47**(2), 024105 (2023) <https://doi.org/10.1088/1674-1137/ac9fb8>
- [204] Bally, B., Giacalone, G., Bender, M.: The shape of gold. *Eur. Phys. J. A* **59**(3), 58 (2023) <https://doi.org/10.1140/epja/s10050-023-00955-3> arXiv:2301.02420 [nucl-th]
- [205] Giacalone, G., et al.: The unexpected uses of a bowling pin: anisotropic flow in fixed-target $^{208}\text{Pb}+^{20}\text{Ne}$ collisions as a probe of quark-gluon plasma (2024) arXiv:2405.20210 [nucl-th]
- [206] Zhang, C., Chen, J., Giacalone, G., Huang, S., Jia, J., Ma, Y.-G.: *Ab-initio* nucleon-nucleon correlations and their impact on high energy $^{16}\text{O}+^{16}\text{O}$ collisions (2024) arXiv:2404.08385 [nucl-th]
- [207] Giacalone, G., Nijs, G., Schee, W.: Determination of the Neutron Skin of Pb208 from Ultrarelativistic Nuclear Collisions. *Phys. Rev. Lett.* **131**(20), 202302 (2023) <https://doi.org/10.1103/PhysRevLett.131.202302> arXiv:2305.00015 [nucl-th]
- [208] Pihan, G., Monnai, A., Schenke, B., Shen, C.: Unveiling Baryon Charge Carriers through Charge Stopping in Isobar Collisions. *Phys. Rev. Lett.* **133**(18), 182301 (2024) <https://doi.org/10.1103/PhysRevLett.133.182301> arXiv:2405.19439 [nucl-th]
- [209] Garcia-Montero, O., Elfner, H., Schlichting, S.: Charge and energy deposition in the McDIPPER framework. *PoS HardProbes2023*, 054 (2024) <https://doi.org/10.22323/1.438.0054> arXiv:2311.03125 [hep-ph]

- [210] Gelfand, D., Ipp, A., Müller, D.: Simulating collisions of thick nuclei in the color glass condensate framework. *Phys. Rev. D* **94**(1), 014020 (2016) <https://doi.org/10.1103/PhysRevD.94.014020> arXiv:1605.07184 [hep-ph]
- [211] Ipp, A., Müller, D.: Broken boost invariance in the Glasma via finite nuclei thickness. *Phys. Lett. B* **771**, 74–79 (2017) <https://doi.org/10.1016/j.physletb.2017.05.032> arXiv:1703.00017 [hep-ph]
- [212] Matsuda, H., Huang, X.-G.: Simulation of a (3+1)D glasma in Milne coordinates: Topological charge, eccentricity, and angular momentum (2024) arXiv:2409.08742 [hep-ph]
- [213] Matsuda, H., Huang, X.-G.: Effect of Longitudinal Fluctuations of 3D Weizsäcker–Williams Field on Pressure Isotropization of Glasma. *Entropy* **26**(2), 167 (2024) <https://doi.org/10.3390/e26020167> arXiv:2401.04296 [physics.plasm-ph]
- [214] Altinoluk, T., Dumitru, A.: Particle production in high-energy collisions beyond the shockwave limit. *Phys. Rev. D* **94**(7), 074032 (2016) <https://doi.org/10.1103/PhysRevD.94.074032> arXiv:1512.00279 [hep-ph]
- [215] Altinoluk, T., Beuf, G., Mulani, S.: Forward parton-nucleus scattering at next-to-eikonal accuracy in the CGC (2024) arXiv:2411.15047 [hep-ph]
- [216] Kharzeev, D., Levin, E., Nardi, M.: The Onset of classical QCD dynamics in relativistic heavy ion collisions. *Phys. Rev. C* **71**, 054903 (2005) <https://doi.org/10.1103/PhysRevC.71.054903> arXiv:hep-ph/0111315
- [217] Kharzeev, D., Levin, E., Nardi, M.: QCD saturation and deuteron nucleus collisions. *Nucl. Phys. A* **730**, 448–459 (2004) <https://doi.org/10.1016/j.nuclphysa.2004.06.022> arXiv:hep-ph/0212316. [Erratum: *Nucl.Phys.A* 743, 329–331 (2004)]
- [218] Gelis, F., Venugopalan, R.: Large mass q anti- q production from the color glass condensate. *Phys. Rev. D* **69**, 014019 (2004) <https://doi.org/10.1103/PhysRevD.69.014019> arXiv:hep-ph/0310090
- [219] Garcia-Montero, O., Schlichting, S., Zhu, J.: Effects of sub-nucleonic fluctuations on the longitudinal structure of heavy-ion collisions (2025) arXiv:2501.14872 [nucl-th]
- [220] Garcia-Montero, O., Schlichting, S.: Baryon stopping and charge deposition in heavy-ion collisions due to gluon saturation (2024) arXiv:2409.06788 [hep-ph]
- [221] Iancu, E., Triantafyllopoulos, D.N.: JIMWLK evolution for multi-particle production in Langevin form. *JHEP* **11**, 067 (2013) [https://doi.org/10.1007/JHEP11\(2013\)067](https://doi.org/10.1007/JHEP11(2013)067) arXiv:1307.1559 [hep-ph]